

ABSTRACT

This report is divided into two parts. The first part is the measurement of heats of mixing at 25°C, for the system carbontetrachloride-tetrachloroethylene; the second part is the investigation of liquid phase adsorption of binary liquid mixtures, using silica gel as the adsorbent.

The heats of mixing for the system carbontetrachloride-tetrachloroethylene were measured as a function of composition; and it is found that this system is a non-ideal one though the deviations from ideality are of smaller order compared with those systems such as benzene-n-pentane and benzene-n-decane⁽²⁾.

Four systems were investigated for liquid phase adsorption, namely, benzene-n-hexane-silica gel, benzene-n-heptane-silica gel, benzene-n-octane-silica gel and benzene-n-decane-silica gel. Adsorption equilibria of the systems were determined at 25°C and 1 atmosphere. Everett's interpretation⁽⁴⁾ was adopted; and with the activity coefficients in the liquid phase evaluated by Lu's method⁽⁵⁾ of extrapolation, the activity coefficients in the adsorbed phase \bar{y}_1, \bar{y}_2 and the separation factor K' were evaluated. The results show that deviations from ideality do exist in the adsorbed phase and that the chain length of the n-alkanes has no effect on the separation factor K' .

ACKNOWLEDGEMENT

The author is indebted to Dr. Benjamin C.Y. Lu, the director of this thesis, for his encouragement, kind assistance and valuable guidance throughout the course of this work.

Special thanks are due to Dr. R.F. Lama, the originator of this particular calorimeter, for his valuable guidance.

TABLE OF CONTENTS

ABSTRACT	i
ACKNOWLEDGEMENT	ii
TABLE OF CONTENTS	iii
LIST OF FIGURES.....	v
LIST OF TABLES	viii
NOMENCLATURE	ix
PART I HEATS OF MIXING OF LIQUIDS.....	1
INTRODUCTION	2
THEORETICAL CONSIDERATIONS	3
LITERATURE SURVEY	6
EXPERIMENTAL DETAILS	9
Materials	9
Preparation of the mixing vessel	10
Loading the mixing vessel	12
Thermal equilibrium	12
The mixing process	15
The calibration	16
Evaluation of experimental data	18
SAMPLE CALCULATION	23
RESULTS	26
DISCUSSIONS	30

PART II	LIQUID PHASE ADSORPTION	35
	INTRODUCTION	36
	LITERATURE SURVEY	38
	THEORETICAL CONSIDERATIONS	47
	EXPERIMENTAL DETAILS	54
	Materials	54
	Preparation of binary mixtures	57
	Loading the adsorption vessel	59
	Equilibrium adsorption	61
	Analysis of the equilibrium mixture	62
	Surface area of the adsorbent	62
	The B.E.T. method	69
	PRESENTATION OF RESULTS	75
	SAMPLE CALCULATION	77
	DISCUSSIONS	85
	CONCLUSIONS	88
	LITERATURE SITED	101
APPENDIX I	Method of extrapolation for activity coefficients in the liquid phase	104
APPENDIX II	The method of evaluation of activity coefficients in the adsorbed phase ..	112

LIST OF FIGURES

<u>FIGURE</u>	<u>TITLE</u>	<u>PAGE</u>
1	The brass mixing vessel	11
2	The brass jacket	13
3	Thermistor circuit	17
4	Heater circuit	17
5	Variation of thermistor resistance in a heat of mixing experiment	19
6	Variation of thermistor resistance in a heat of mixing experiment	19
7	Heats of mixing data at 25°C for the system carbontetrachloride-tetrachloroethylene ..	29
8	Heats of mixing values predicted by using solubility parameters for the system carbontetrachloride-tetrachloroethylene ..	33
9	The degassing oven	56
10	The brass desiccator	60
11	The nitrogen adsorption apparatus	68
12	Surface area measurement, a plot of $\frac{P/P_c}{w^s(1-P/P_c)}$ against p/p_0	74
13	Equilibrium adsorption at 25°C for the system benzene-n-hexane-silica gel. A plot of $x_1^L x_2^L / (n^0 \frac{\Delta x_1^L}{m})$ vs. x_1^L	90

14	Equilibrium adsorption at 25°C for the system benzene-n-heptane-silica gel. A plot of $x_1^l x_2^l / (n^0 \frac{\Delta x_1^l}{m})$ vs. x_1^l	91
15	Equilibrium adsorption at 25°C for the system benzene-n-octane-silica gel. A plot of $x_1^l x_2^l / (n^0 \frac{\Delta x_1^l}{m})$ vs. x_1^l	92
16	Equilibrium adsorption at 25°C for the system benzene-n-decane-silica gel. A plot of $x_1^l x_2^l / (n^0 \frac{\Delta x_1^l}{m})$ vs. x_1^l	93
17	Equilibrium $x_1^\sigma - x_1^l$ diagram for the system benzene-n-hexane-silica gel at 25°C.....	94
18	Equilibrium $x_1^\sigma - x_1^l$ diagram for the system benzene-n-heptane-silica gel at 25°C.....	95
19	Equilibrium $x_1^\sigma - x_1^l$ diagram for the system benzene-n-octane-silica gel at 25°C	96
20	Equilibrium $x_1^\sigma - x_1^l$ diagram for the system benzene-n-decane-silica gel at 25°C	97
21	Calculated $\ln \bar{Y}^\sigma$ values as a function of x_1^σ for the system benzene-n-hexane-silica gel	98
22	Calculated $\ln \bar{Y}^\sigma$ values as a function of x_1^σ for the system benzene-n-heptane-silica gel	99
23	Calculated $\ln \bar{Y}^\sigma$ values as a function of x_1^σ for the system benzene-n-octane-silica gel	100
24	Heats of mixing data for the system benzene-n-heptane at 25°C. A plot of $\Delta \tilde{H}^M$ vs. x_1	108
25	A plot of $\ln \bar{Y}$ against x_1 for the system benzene-n-heptane at 60°C	109

26	A plot of $\ln \gamma$ against x_1 for the system benzene-n-heptane at 80°C	110
27	A plot of $\ln \gamma$ against x_1 for the system benzene-n-heptane at 25°C (calculated values)	111
28	Calibration curve on refractive indices for the system benzene-n-heptane at 25°C	63
29	A comparison of the excess enthalpy of mixing with the excess free energy of mixing for the system carbontetrachloride-tetrachloroethylene at 25°C	34

26	A plot of $\ln \gamma$ against x_1 for the system benzene-n-heptane at 80°C	110
27	A plot of $\ln \gamma$ against x_1 for the system benzene-n-heptane at 25°C (calculated values)	111
28	Calibration curve on refractive indices for the system benzene-n-heptane at 25°C	63
29	A comparison of the excess enthalpy of mixing with the excess free energy of mixing for the system carbontetrachloride-tetrachloroethylene at 25°C	34

LIST OF TABLES

<u>TABLE</u>	<u>TITLE</u>	<u>PAGE</u>
1	Heats of mixing data at 25°C for the system carbontetrachloride-tetrachloroethylene	27
2	Values of solubility parameter for carbon-tetrachloride obtained from various methods	28
3	Physical properties of pure liquids	58
4	Calibration data on refractive indices	64,65
5	Equilibrium adsorption data at 25°C for the system benzene-n-hexane-silica gel	81
6	Equilibrium adsorption data at 25°C for the system benzene-n-heptane-silica gel ...	82
7	Equilibrium adsorption data at 25°C for the system benzene-n-octane-silica gel	83
8	Equilibrium adsorption data at 25°C for the system benzene-n-decane-silica gel	84
9	Extrapolation of activity coefficients for the system benzene-n-heptane at 25°C	107
10	Values for evaluating the activity coefficients in the adsorbed phase	114

NOMENCLATURE

a, b, c	constants
$\Delta \tilde{E}^M$	molal energy of mixing, in cal./mole
$\Delta \tilde{E}^V$	molal energy of vaporization, in cal./mole
\tilde{H}	molal enthalpy of a solution at a certain temperature and pressure
\bar{H}_i	partial molar enthalpy of component i in a solution
ΔH	heat change, in calories
$\Delta \tilde{H}^E$	molal excess heat of mixing, in cal./mole
$\Delta \tilde{H}^M$	heat of mixing per mole of solution, in cal./mole
$\Delta \tilde{H}_{ideal}^M$	molal heat of mixing for an ideal solution, in cal./mole
ΔH^V	enthalpy of vaporization, in cal./gm.
i	current, in amperes
j	the electrical equivalent of heat, 4.184 joules/cal
K	separation factor for a perfect system
K'	separation factor for a real system
K_1, K_2, K_3, K_4	constants
k	constant
M	molecular weight of a substance, in grams
m	number of grams of a substance

n	number of moles of a substance
n_D^{25}	refractive index of a liquid at 25° C
P	pressure, in mm Hg
P_0	atmospheric pressure, 760 mm Hg
$\frac{dQ}{dt}$	the rate of heat supply to the calorimeter, in cal./sec.
R	resistance, in ohms
R_s	the resistance of the standard resistor, in ohms
r	weight fraction
ΔR	change of resistance, in ohms
\tilde{V}	molal volume of a substance
\tilde{V}_l	molal volume of a liquid, in cc/mole
V_s	the potential drop across the standard resistor, in volts
V^σ	adsorptive capacity, in cc/gm.
W	weight, in grams
W_m	the mass of nitrogen adsorbed on W grams of silica gel
x	mole fraction
Δx_1^l	defined as $x_1^\sigma - x_1^l$
α, β	constants
γ	activity coefficient
Γ	absolute magnitude of adsorption, in moles/m ²

θ	time, in seconds
δ	solubility parameter
ρ	density, in gm./cc.
ϕ	volume fraction
$\bar{\Phi}$	area occupied per mole of a component
Σ_s	surface area of a substance, in m ² /gm.
log	logarithm based on e

superscripts:

\circ	in the original solution
l	liquid phase
(G)	with respect to weight
g	gas phase
(N)	with respect to the number of moles
(V)	with respect to volume
σ	in the adsorbed phase

subscripts:

i	component i
l	liquid
1,2	components 1 or 2

PART I

Heats of mixing of liquids

INTRODUCTION

The binary system carbontetrachloride-tetrachloroethylene had been investigated previously⁽¹⁾ and was considered "nearly ideal" because the activity coefficients evaluated from the experimental isobaric vapor-liquid equilibrium data "distributed around unity".

If this information is considered in terms of excess thermodynamic properties,

$$H^E = G^E + T S^E$$

where H^E is the excess enthalpy; S^E is the excess entropy and G^E is the excess free energy of mixing, which is closely related to the activity coefficients, we may have a better understanding about this system. Since the G^E evaluated from the reported experimental data are scattering, as shown in Fig.29,P.34, it is desirable to obtain experimental data on heats of mixing so that the H^E term will help to show whether this system is athermal, regular or ideal.

Brass calorimeters of the same type as used by Lama and Lu⁽¹³⁾, were used for the measurements. This calorimeter had been used to measure heats of mixing for some systems^{(13),(2)} with acceptable results.

THEORETICAL CONSIDERATIONS

The heat effect produced on mixing two pure components, under the same temperature and pressure, is called the "integral heat of solution" or simply "heat of mixing", which is designated as $\Delta\tilde{H}^M$. This thermal effect is stated on the basis of one mole of the resulting solution.

For an ideal binary system, the molal enthalpy of the solution is defined as

$$\tilde{H} = x_1 \tilde{H}_1 + x_2 \tilde{H}_2 \quad (1)$$

where \tilde{H} is the molal enthalpy of the solution; \tilde{H}_1 and \tilde{H}_2 are the molal enthalpies of the pure components 1 and 2 respectively, at the same temperature and pressure; and x_1 , x_2 are the mole fractions of the components 1 and 2 respectively, in the solution.

For a real system, the heat of mixing has to be considered, hence

$$\tilde{H} = x_1 \tilde{H}_1 + x_2 \tilde{H}_2 + \Delta\tilde{H}^M \quad (2)$$

where $\Delta\tilde{H}^M$ is the heat of mixing per mole of solution,

and is considered positive for endothermic process when heat is absorbed by the system.

If we designate the heat of mixing as the enthalpy difference between the final and initial states of a mole of the solution at constant temperature and pressure, then we have

$$\Delta \tilde{H}^M = \underset{\substack{\text{final} \\ \text{state}}}{\tilde{H}} - (n_1 \underset{\substack{\text{initial} \\ \text{state}}}{\tilde{H}_1} + n_2 \tilde{H}_2) \quad (3a)$$

applying Euler's theorem, on one mole basis,

$$\begin{aligned} \tilde{H} &= x_1 \frac{\partial H}{\partial n_1} + x_2 \frac{\partial H}{\partial n_2} \\ &= x_1 \bar{H}_1 + x_2 \bar{H}_2 \end{aligned} \quad (3b)$$

where \bar{H}_1 and \bar{H}_2 are defined as the partial molar enthalpies of components 1 and 2 respectively. They represent the change in enthalpy of a very large quantity of the solution when one mole of the pure components 1 or 2 respectively, is added at constant temperature and pressure.

Combining (3a) and (3b),

$$\Delta \tilde{H}^M = x_1 (\bar{H}_1 - \tilde{H}_1) + x_2 (\bar{H}_2 - \tilde{H}_2) \quad (4)$$

the heat of mixing might be expressed in terms of partial molar enthalpies and molar enthalpies of the pure components.

An excess property is defined as the difference between the actual property and the property which one would obtain for an ideal solution at the same conditions. Therefore the excess heat of mixing is expressed as ,

$$\tilde{H}^E = \underset{\text{real}}{\Delta \tilde{H}^M} - \underset{\text{ideal}}{\Delta \tilde{H}^M} \quad (5)$$

where \tilde{H}^E is the excess heat of mixing per mole of solution; $\Delta \tilde{H}^M_{\text{real}}$ is the molal heat of mixing for a real system and $\Delta \tilde{H}^M_{\text{ideal}}$ is the molal heat of mixing for an ideal solution.

From equation (5), it is obvious that the excess molal enthalpy of mixing, \tilde{H}^E , is equal to the integral enthalpy of mixing per mole of solution, $\Delta \tilde{H}^M$, because the enthalpy of mixing for an ideal solution is zero.

LITERATURE SURVEY

The measurements of heats of mixing have always been considered difficult operations. The use of calorimeters is the main factor of such measurements. Various kinds of calorimeters have been used by different researchers, and each type has been found to be successful to some extent. Among the great number of calorimeters previously used, the main types and the more important ones are briefly discussed below:

Adiabatic calorimeter by Richards⁽⁶⁾ This was used as early as 1905. In this calorimeter the heat losses due to radiation were minimized by keeping the temperature of the calorimeter content at the same level as that of the ambient atmosphere.

Special calorimeter for heats of solution and heats of mixing This was started in 1930. All those used by Carroll and Mathews⁽⁷⁾, by Macleod and Wilson⁽⁸⁾ and by Void⁽⁹⁾ were of the various forms of the ordinary Dewar flask type for isothermal measurements.

Calorimeter used by Scatchard et. al.⁽¹⁰⁾ In 1952, they used the new form of externally agitated calorimeter.

It consisted of a horseshoe-shaped tube in which mercury was used initially to separate the two components, and was then used to enhance the mixing process.

Tsao and Smith apparatus.⁽¹¹⁾ A vacuum Dewar flask was used as the body of the calorimeter. A second component was added to the first one by a jacketed burette. This arrangement permitted very rapid and relatively accurate determinations to be carried out at constant temperature, but compensations still had to be made for "radiation effects".

Calorimeter used by Hanson and Van Winkle⁽¹²⁾ in 1960. This was the similar type as that used by Murti and Van Winkle; but thermocouples were used to measure the temperature variations. The mode of calculations involved the determination of the heat capacity of the calorimeter and contents, and seemed to yield reliable results.

Isothermal dilution calorimeter.⁽³⁶⁾ This was used by Van Ness and his co-workers in 1966, for the measurement of endothermic heats of mixing. It consisted mainly of a Dewar flask and a feed bulb. Components were fed into the flask by using mercury displacement, and electrical energy was supplied to maintain constant temperature.

Measurements could be operated at low mole fractions and the estimated error was only $\pm 1\%$.

EXPERIMENTAL DETAILS

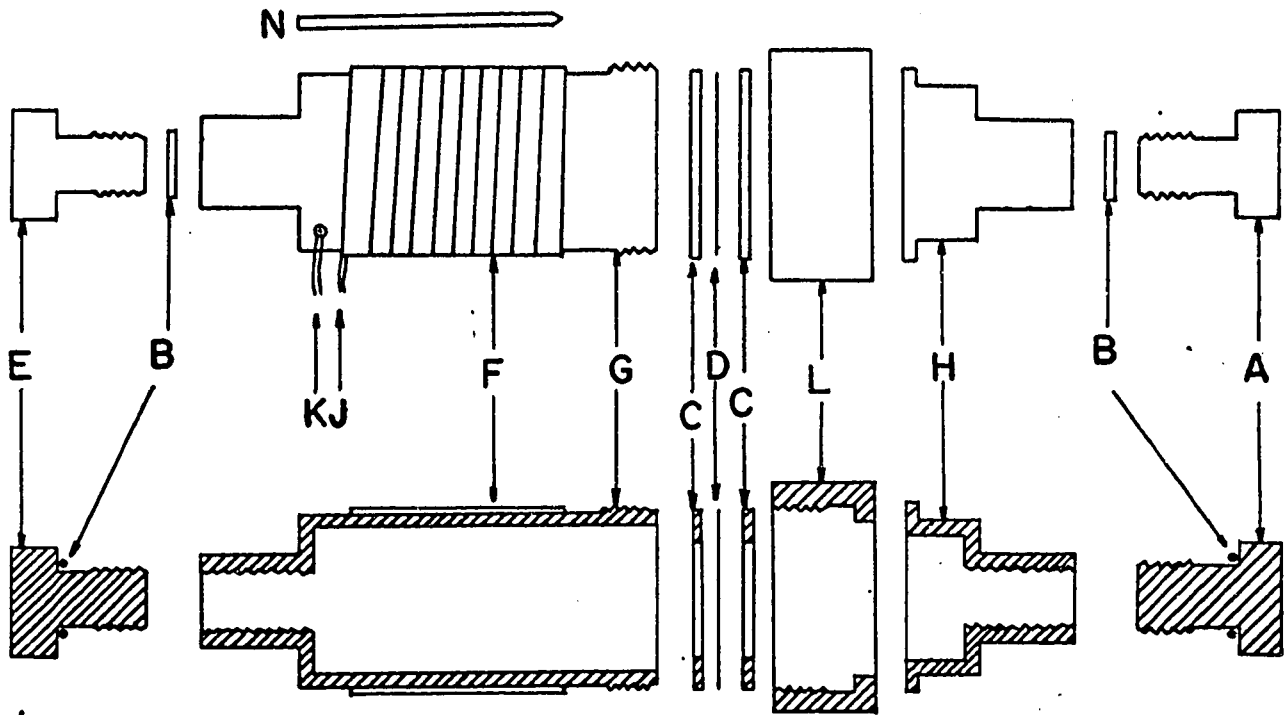
MATERIALS

The liquid carbontetrachloride and tetrachloroethylene used in this investigation were both of spectro-grade and were supplied by Coleman and Bell Co. The refractive indices were measured as 1.45712 and 1.50296 for carbontetrachloride and tetrachloroethylene respectively, and were considered in good agreement with the literature (18), which listed the values as 1.45704 and 1.50284 for carbontetrachloride and tetrachloroethylene respectively. The materials were used directly from the manufacturer without any further purification.

PREPARATION OF THE MIXING VESSEL

Brass mixing vessels with volumes varying from 10 cc to 14 cc were used for the measurement of heats of mixing. One of these mixing vessels is shown schematically in Fig.1. It was divided into 2 compartments that screwed into each other. The two compartments were separated by a 0.0015 inch tin-foil diaphragm placed in between two teflon gaskets. Each compartment had a filling opening closed by an o-ring and a brass plug. A manganin wire was wound non-inductively on the outside surface of the lower compartment to work as a heater, and was coated with Glyptal resin. A thermistor was cemented onto the external surface of the lower compartment by using Epoxy cement. A gold-plated nail was placed inside the mixing vessel.

First, the mixing vessel was tested for leakage. The upper compartment was filled with petroleum ether and the upper plug was screwed in place. This was put into a glass desiccator equipped with active silica gel and evacuated to 10^{-2} mm Hg by a vacuum pump. A constant weight after repeated evacuations indicated that there was no leakage. The same procedure was performed to test the lower compartment.



- A upper plug
- B o-rings
- C teflon gaskets
- D tin foil
- E lower plug
- F mixing vessel heater
- G lower compartment
- H upper compartment
- J leads of the mixing vessel heater
- K leads of the thermistor
- L the ring to join the two compartments together
- N gold-plated nail

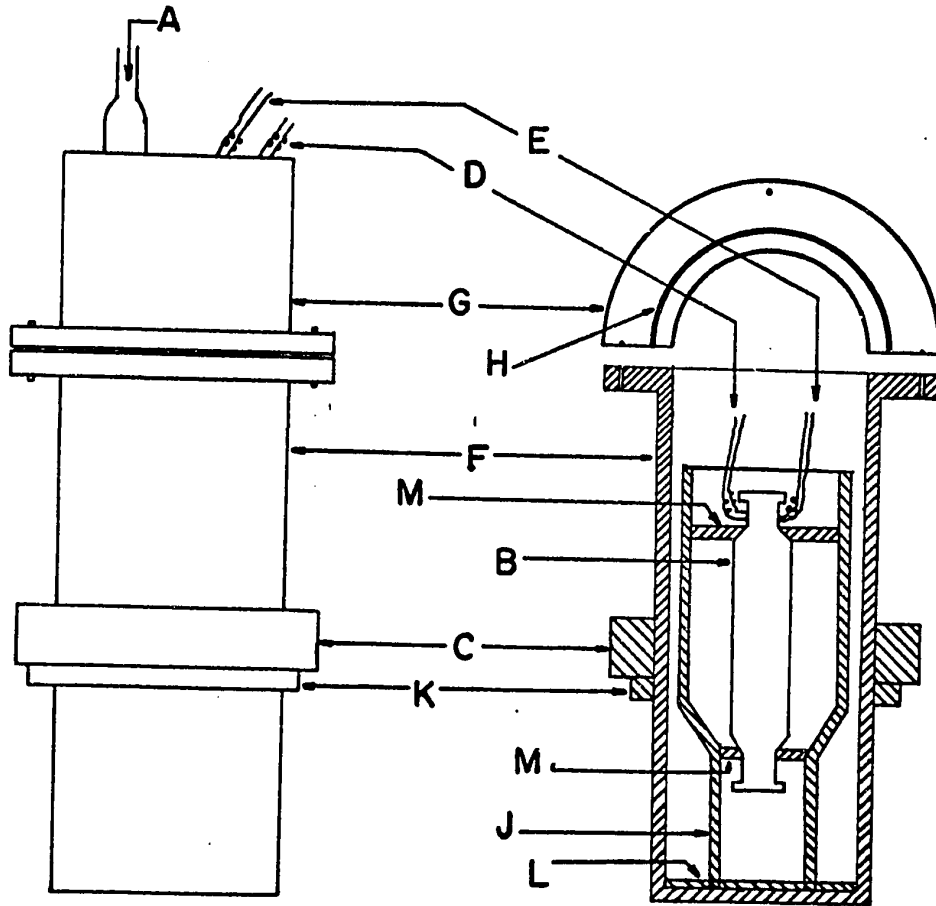
Fig. 1 The brass mixing vessel

LOADING THE MIXING VESSEL

When no leakage was detected, the petroleum ether was removed and the mixing vessel was dried under vacuum in the desiccator for 1 hour. Then the weight of the empty mixing vessel, together with the gold-plated nail, was obtained from an analytical balance, reading to 10^{-4} gram. The upper compartment was filled with liquid component 1 and the upper plug was quickly screwed in. After a dry nitrogen purge and 20 minutes' drying in the desiccator, the mixing vessel and its contents were weighed again. The difference of the two weighings gave the amount of liquid component 1 in the vessel. The same procedure was performed to obtain the weight of liquid component 2 in the vessel.

THERMAL EQUILIBRIUM

The loaded mixing vessel was then put into the brass jacket as shown schematically in fig.2. The jacket was a long brass cylinder about 3 in. O.D., and 24 inches in length. Rings of styrofoam and plexiglass were used to keep the vessel from getting into contact with the



- | | | | |
|---|-------------------|---|--------------------------|
| A | to vacuum | D | leads of the heater |
| B | the mixing vessel | E | leads of the thermistor |
| C | solenoid | F | lower part of the jacket |
| H | o-ring | G | upper part of the jacket |
- J rubber tubing used to support the mixing vessel
K brass ring for supporting the solenoid
L pieces of insulation for adjusting the proper position of the vessel such that the solenoid could energize the nail
M rings of plexiglass and styrofoam for keeping the vessel from getting into contact with the jacket

Fig. 2 The brass jacket

jacket. Its inside wall was polished to shining and a vacuum system was connected to the jacket so that heat losses due to conduction, convection and radiation were brought to a minimum. A solenoid was installed outside the jacket. It was used to energize the nail to work as a stirrer. It obtained its power supply from four twelve-volts lead-acid storage batteries connected in series. A motor with cam-actuated shaft was used to operate a microswitch such that 30 times per minute of opening-closing operations were obtained.

The brass jacket, together with its contents, was immersed into a water bath. The water bath was a glass tank of 30"x15"x20" , which was set in a wooden box, with styrofoam lagging between them. Two immersion heaters of 750 watts each were used to supply heat, and four cooling coils were used for cooling. Two stirrers provided efficient circulation throughout the bath, and a controller was used to maintain constant temperature in the bath at $25 \pm 0.005^{\circ}\text{C}$. A Beckman thermometer was used to read the temperature fluctuation in the bath. This fluctuation was found to be $\pm 0.005^{\circ}\text{C}$. The bath was installed in a room of $25 \pm 1^{\circ}\text{C}$ controlled by an air-conditioner. At least eight hours were allowed for reaching thermal equilibrium.

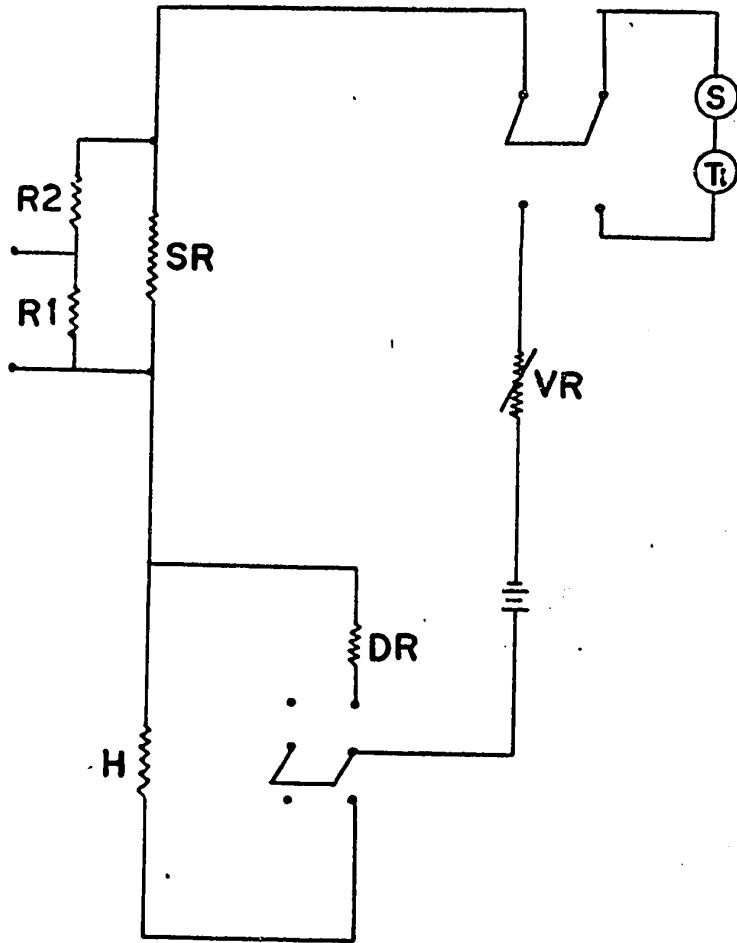
THE MIXING PROCESS

When thermal equilibrium was reached, as indicated by a constant value of the thermistor resistance. The solenoid circuit was closed such that the nail inside the mixing vessel was energized and started moving up and down. About 2 minutes later, the tin foil was broken as indicated by point A in fig.5, in which a typical recording chart was drawn as an illustration. When the mixing process was started, the temperature of the mixing vessel changed and was indicated by changes of the thermistor resistance. This was illustrated as AD in fig.5. The thermistor circuit was shown in fig. 3. The leads from the thermistor (Th) were connected to a Wheatstone Bridge (Tinsley & Co. type 4970). A 2-volts lead-acid storage battery was used as the power supply. When the resistance of the thermistor varied due to a change of temperature, the Bridge equilibrium was disturbed. The output from the Wheatstone Bridge was fed to the electronic D-C Null-Detector. The amplified D.C. voltage drove a 50 mv. recorder with a chart speed of one inch per minute. The sensitivity of the circuit was such that a change of 4 mv. corresponded to a change of temperature of about 0.001°C.

As the endothermic mixing process was completed, about 10 minutes were allowed to obtain a constant "warming" rate, as shown by DB in fig.5.

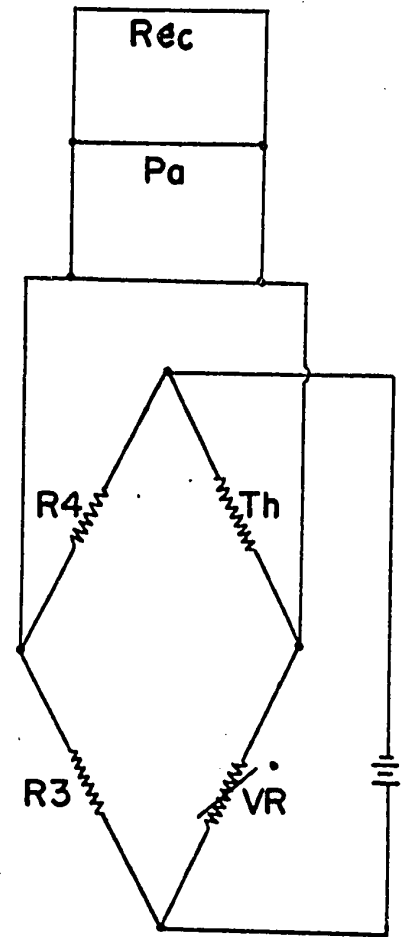
THE CALIBRATION

About 10 minutes after the endothermic mixing process was completed, the heater circuit was closed such that the mixing vessel and its contents were heated up to approximately the original temperature, indicated by the thermistor resistance. About 10 minutes was also allowed to obtain a constant "cooling" rate as indicated by NL in fig.5. During the heating period, the potential drop across a standard resistor was recorded. The heating circuit was shown in fig.4. A 6-volts lead-acid storage battery was used as the power supply. A variable resistor (VR) allowed adjustment of the circuit potential. The current through the heater (H) could be calculated from the measured potential drop across a standard resistor (SR). This potential drop was determined by measuring a portion of the potential from a volt box having a nominal ratio, $R_1/(R_1+R_2)$, of 1 to 10. The potential measurements were performed with a k-3 potentiometer in conjunction with a high sensitivity galvanometer. The heater resistance which



R₁ 300 ohms resistance
R₂ 3000 ohms resistance
VR variable resistance
SR standard resistance
DR dummy resistor
H mixing vessel heater

Fig. 4 Heater circuit



R₃ 1000 ohms resistance
R₄ 1000 ohms resistance
Th thermistor
Pa preamplifier
Rec recorder
Ti electric timer

Fig.3 Thermistor circuit

included a 10 cm. of thermocouple wire No.3c, was also measured on the Wheatstone Bridge. The heating time was measured to 0.05 seconds by a Precision electric timer (Ti) operated by the power main supply, at a frequency of 60 cycles per second, and was synchronized with the calorimeter heater circuit.

During non-heating periods, the battery was discharged through a dummy resistor (DR), which had a resistance equivalent to that of the mixing vessel heater plus leads. The working cell for the potentiometer was a 2-volts, lead-acid storage battery. The standard cell was certified by the Division of Applied Physics of National Research Council of Canada.

EVLUATION OF EXPERIMENTAL DATA

The temperature change of the mixing vessel due to the mixing process was measured in terms of resistance change of the thermistor. A calibration was performed such that a measured amount of electricity would produce the same resistance change. Hence by comparison the heat of mixing could be calculated.

To illustrate the evaluation of experimental data,

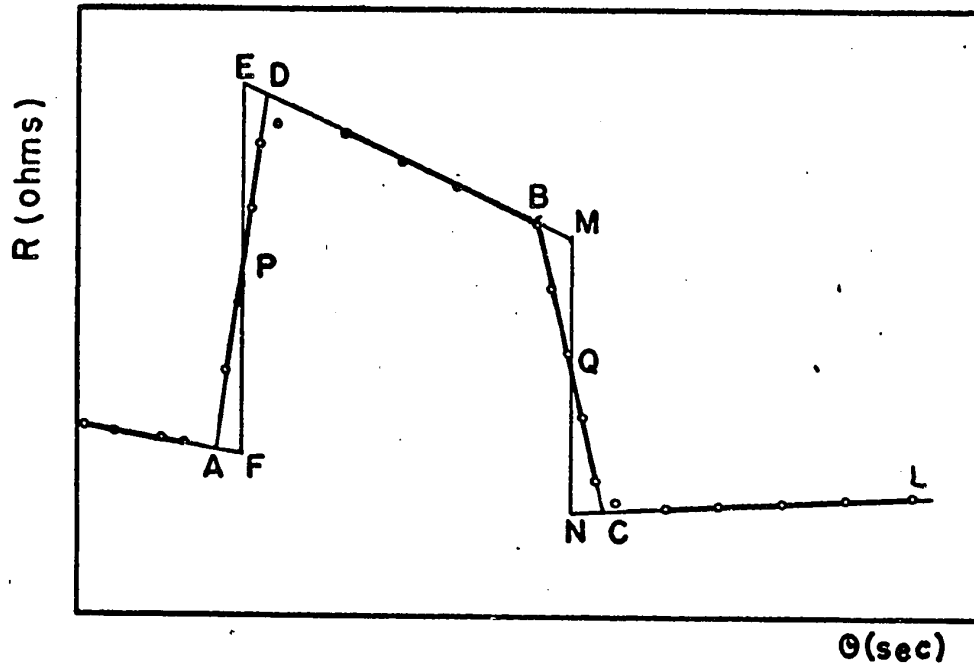


Fig.5 Variation of thermistor resistance in a heat of mixing experiment

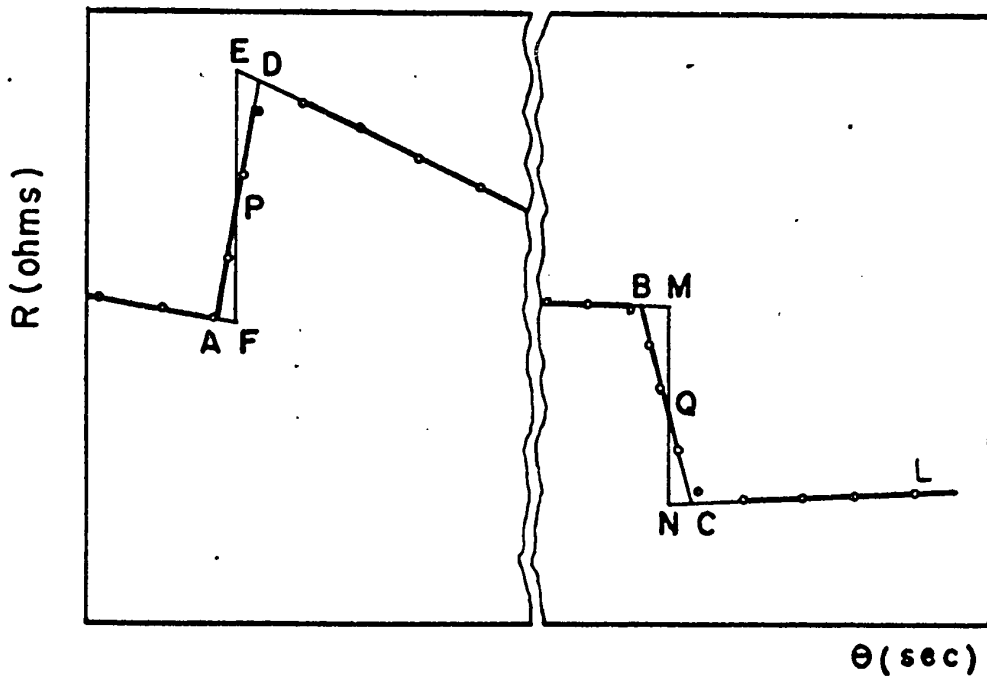


Fig.6 Variation of thermistor resistance in a heat of mixing experiment

a typical experimental recording for endothermic systems was shown in fig.5. At zero time, the nail was energized to move up and down inside the mixing vessel. For the first two minutes, the resistance of the thermistor decreased slightly due to the stirring effect before the foil was broken and before the mixing was started. At point A, the foil was broken and mixing process began. The system cooled down and hence the resistance increased rapidly. When mixing was completed, the temperature began to increase at a constant rate and hence the decrease of resistance was linear, shown as DB.

During the calibration the starting point was at point B, shown in fig.5. Current was supplied to the heater such that the temperature would go back to approximately the original temperature, point C. At this point the heater was turned off and the system cooled down at a constant rate, shown as CL, in fig.5.

The increment of resistance during the run was ΔR_1 , which was calculated by extrapolating the two rating periods AD and BD. It could be proved⁽³⁹⁾ that EF represented the best estimation of the act-

ual ΔR_1 . EF was obtained by using P, the mid-point of DA, for the extrapolation of BD and AF. For the same reason, MN was estimated as the actual decreased resistance ΔR_2 during the calibration, in which heat was supplied through the heater.

The heat supplied to the calorimeter was calculated by using Joule's Law :

$$\begin{aligned}\frac{dQ}{dt} &= \frac{1}{j} i^2 R \\ &= \frac{1}{j} \left(\frac{V_s}{R_s} \right)^2 R_h\end{aligned}$$

where $\frac{dQ}{dt}$ is the rate of heat supplied to the calorimeter (cal./sec.)

V_s is the potential drop across the standard resistor (volts)

R_s is the resistance of the standard resistor (ohms)

R_h is the resistance of the vessel heater (ohms)

j is the electrical equivalent of heat (4.184 joules/cal.)

An alternative method could be used for the electrical calibration. This was shown in fig.6. The same principle as discussed previously was used; except that after the mixing process, the system was allowed to come back to the original temperature. Then heat was supplied to cause approximately the same amount of temperature change indicated by the resistance change of the thermistor and thus enabled the calculation of the heats of mixing. This method required much more time because about 8 hours were required for the system to come back to the original temperature. But this method served as a stand-by method to ensure a calibration for a mixing process.

SAMPLE CALCULATION

Run No.5 was taken as an example to illustrate the procedures of calculations.

WEIGHINGS

A = body of vessel + lower plug82.4253 gm.
B = carbontet. + A93.3049 gm.
upper plug15.6320 gm.
C = tetrachloroethylene + upper plug + B ...118.6334 gm.

carbontetrachloride = B - A10.8796 gm.
tetrachloroethylene = C - B - upper plug 9.6965 gm.

substances	carbontet.	tetrachloro.	total
liquid used (gm)	10.8796	9.6965	
M.Wt. (gm)	153.838	165.848	
gm. moles of liquid used	0.07073	0.05846	0.12919
density (gm/cc)	1.58429	1.61446	
volume (cc)	6.8672	6.0060	12.8732
x, mole fr.	0.5474	0.4526	1.0000
ϕ , vol. fr.	0.5334	0.4666	1.0000
x_1x_2	0.2478		
$\phi_1\phi_2$	0.2489		
cc/mole	99.647		

ELECTRICAL CALIBRATION

θ = heating time62.7 sec.
 V_s = voltage drop across the standard resistor 4.1867 volts
 R_s = standard resistor 39.492 ohms
 R = mixing vessel heater 13.651 ohms
 $\frac{1}{J}$ = 1/4.184 0.239
 i = current = $V_s/R_s = 4.1867/39.492$ 0.1060 amp.
 dQ = calories supplied by the heater
 = $\frac{1}{J} i^2 R \theta$ 2.2990 cal.
 ΔR_2 = change of resistance in calibration .. 12.21 ohms
 ΔR_1 = change of resistance in the run 10.83 ohms
 ΔH = heat absorbed during mixing process
 = $\frac{R_1}{R_2} dQ = (10.83/12.21) (2.2990)$ 2.0392 cal.
 $\Delta \tilde{H}^M$ = heat of mixing per mole of mixture 15.78 cal/M.
 $\Delta \tilde{H}^M/x_1x_2 = 15.78/0.4287$ 63.70 cal/M.

SOLUBILITY PARAMETER

The solubility parameter of tetrachloroethylene was calculated by using energy of vaporization data⁽¹⁸⁾, at 25°C.

tetrachloroethylene

$$M.Wt. = 165.848 \text{ gm.}$$

$$\rho = 1.61446 \text{ gm./cc.}$$

$$\Delta H_{25}^V = 57.1 \text{ cal./gm.}$$

$$\Delta \tilde{E}_{25}^V \approx \tilde{\Delta H}_{25}^V = (57.1)(165.848) = 9469.9 \text{ cal./mole}$$

$$\tilde{V}_l = M.Wt./\rho = 165.848/1.61446 = 102.7266 \text{ cc./mole}$$

$$\frac{\Delta \tilde{E}^V}{\tilde{V}_l} = 9469.9/102.7266 = 92.2 \text{ cal./cc.}$$

$$\delta_2 = \sqrt{\frac{\Delta \tilde{E}^V}{\tilde{V}_l}} = \sqrt{92.2} = 9.60$$

carbontetrachloride

The solubility parameter of carbontetrachloride was calculated by using equation (9):

$$\Delta \tilde{H}^M = \tilde{V}_m (\delta_1 - \delta_2)^2 \phi_1 \phi_2$$

$$\text{where } \Delta \tilde{H}^M = 15.78 \text{ cal./mole}$$

$$\tilde{V}_l = 102.7266 \text{ cc./mole}$$

$$\delta_2 = 9.60$$

$$\phi_1 \phi_2 = 0.2489$$

$$\text{therefore } \delta_1 = 8.81$$

RESULTS

The heats of mixing values obtained at 25°C for the binary system carbontetrachloride-tetrachloroethylene are listed in Table 1 and are presented graphically in fig.7.

Table 1

HEATS OF MIXING AT 25°C

SYSTEM CARBONTETRACHLORIDE(1)-TETRACHLOROETHYLENE(2)

<u>Run No.</u>	x_1	$\Delta \tilde{H}^M$ expt. <u>cal/mole</u>	δ_1	$\Delta \tilde{H}^M$ calc. <u>cal/mole</u>
1	0.1188	5.10	8.90	6.64
2	0.1803	7.57	8.88	9.23
3	0.3226	12.26	8.85	13.76
4	0.4556	15.30	8.82	15.73
5	0.5474	15.78	8.81	15.79
6	0.7091	14.96	8.76	13.27
7	0.7987	12.26	8.74	10.40
8	0.9040	7.28	8.70	5.65

Table 2

VALUES OF SOLUBILITY PARAMETER OF CARBONTETRACHLORIDE
OBTAINED FROM VARIOUS METHODS (17)

<u>Method used</u>	<u>Solubility parameter, δ,</u>
Heat of vaporization	8.62
Hildebrand rule	8.6
Internal pressure	8.9
Critical constants	8.4
Surface tension	8.65

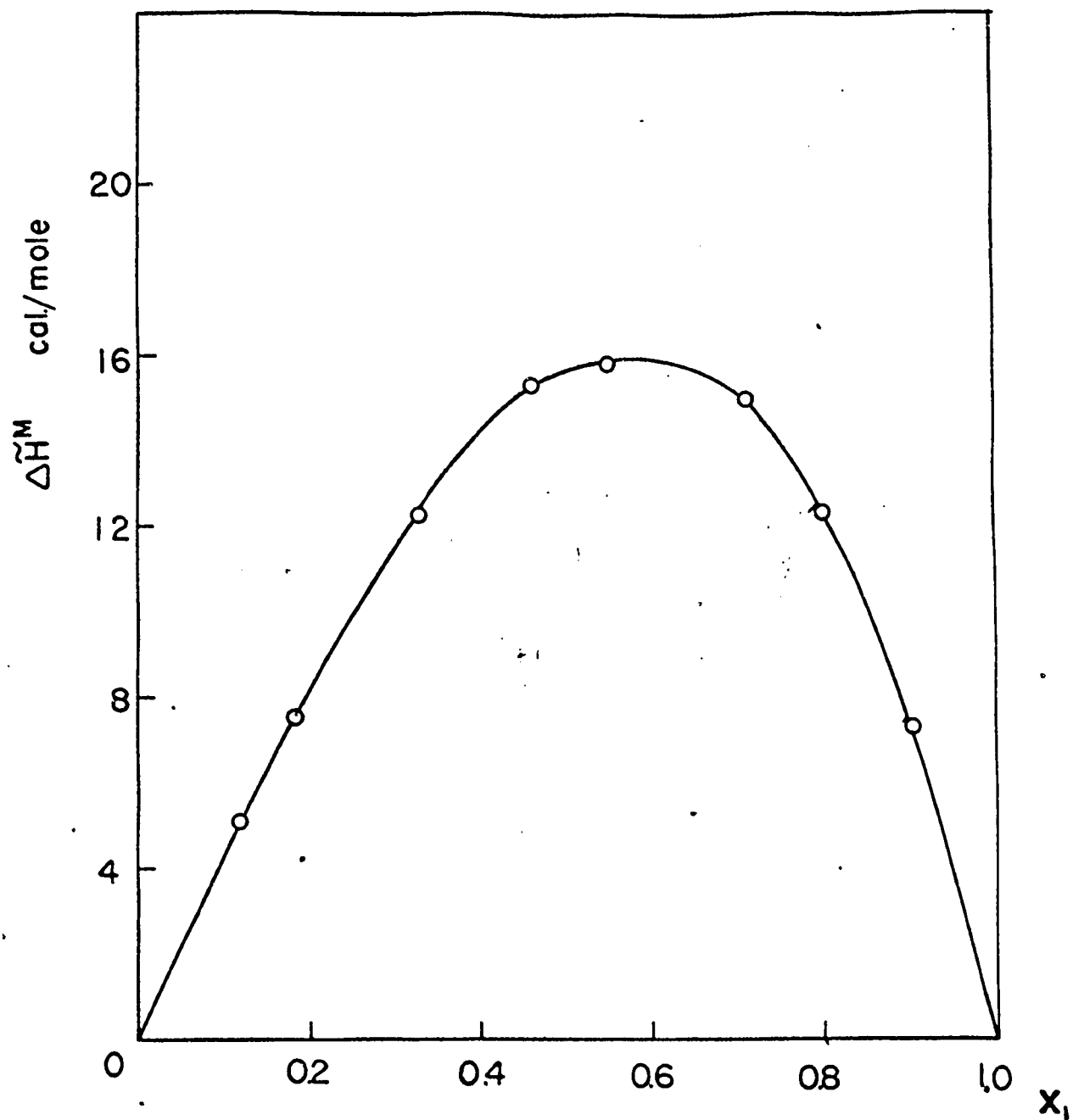


fig.7 Heats of mixing data at 25°C for the system carbontetrachloride-tetrachloroethylene.

DISCUSSIONS

As indicated in fig.7, the values of heats of mixing for the liquid binary system carbontetrachloride-tetrachloroethylene are small compared with those systems such as benzene-n-pentane and benzene-ndecane⁽²⁾, which were found to have values for heats of mixing in the order of 250 cal./mole.

Although small in magnitude, the heats of mixing data obtained are self-consistent. When the excess free energy of mixing is calculated by using the vapor-liquid equilibrium data; and compared with the excess enthalpy of mixing, which is equal to the integral enthalpy of mixing, as shown in fig.29, it is obvious that \tilde{H}^E is not equal to \tilde{G}^E for this system; and that the value of \tilde{G}^E is not very small (in the order of 100 cal./mole). This suggests that this system is not very ideal, and the imperfectness is due to both the effects of heats of mixing and of entropy of mixing.

Hildebrand⁽¹⁶⁾ defined a factor called solubility parameter, in terms of energy of vaporization:

$$\delta = (\Delta \tilde{E}^V / \tilde{V}_l)^{1/2} \quad (7)$$

where $\Delta \tilde{E}^V$ is the molal energy of vaporization at zero pressure, in cal/mole,
 \tilde{V}_l is the molal volume of the liquid, in cc/mole,
 δ is the solubility parameter of the pure substance.

He also related the solubility parameters of the pure components of a mixture with the molal energy of mixing. For a binary mixture, the relation is:

$$\Delta \tilde{E}^M = \tilde{V}_m (\delta_1 - \delta_2)^2 \phi_1 \phi_2 \quad (8)$$

where $\Delta \tilde{E}^M$ is the energy of mixing per mole of mixture,
 \tilde{V}_m is the molal volume of the mixture,
 δ_1, δ_2 are the solubility parameters of pure components 1 and 2 respectively,
 ϕ_1, ϕ_2 are the volume fractions of components 1 and 2 respectively.

When the volume change on mixing is small, the energy of mixing may be expressed by the heat of mixing,

as a close approximation. Hence,

$$\Delta \tilde{H}^M = \tilde{V}_m (\delta_1 - \delta_2)^2 \phi_1 \phi_2 \quad (9)$$

where the $\Delta \tilde{H}^M$ is the molal enthalpy of mixing.

Using equation (9), the experimental data of $\Delta \tilde{H}^M$ were used, together with the solubility parameter of tetrachloroethylene, δ_2 , (calculated by using equation 7 as shown in the sample calculation), to predict δ_1 , the solubility parameter of carbontetrachloride. The calculated values of δ_1 are listed in Table 1. They were found in good agreement with existing values⁽¹⁷⁾ as shown in Table 2.

However, when using the average value (8.804) of the calculated values, together with the same δ_2 (9.602), equation (9) gives values of $\Delta \tilde{H}^M$ close to the experimental data but with some discrepancy, as shown in fig.8. This serves as a test of the applicability of equation (9).

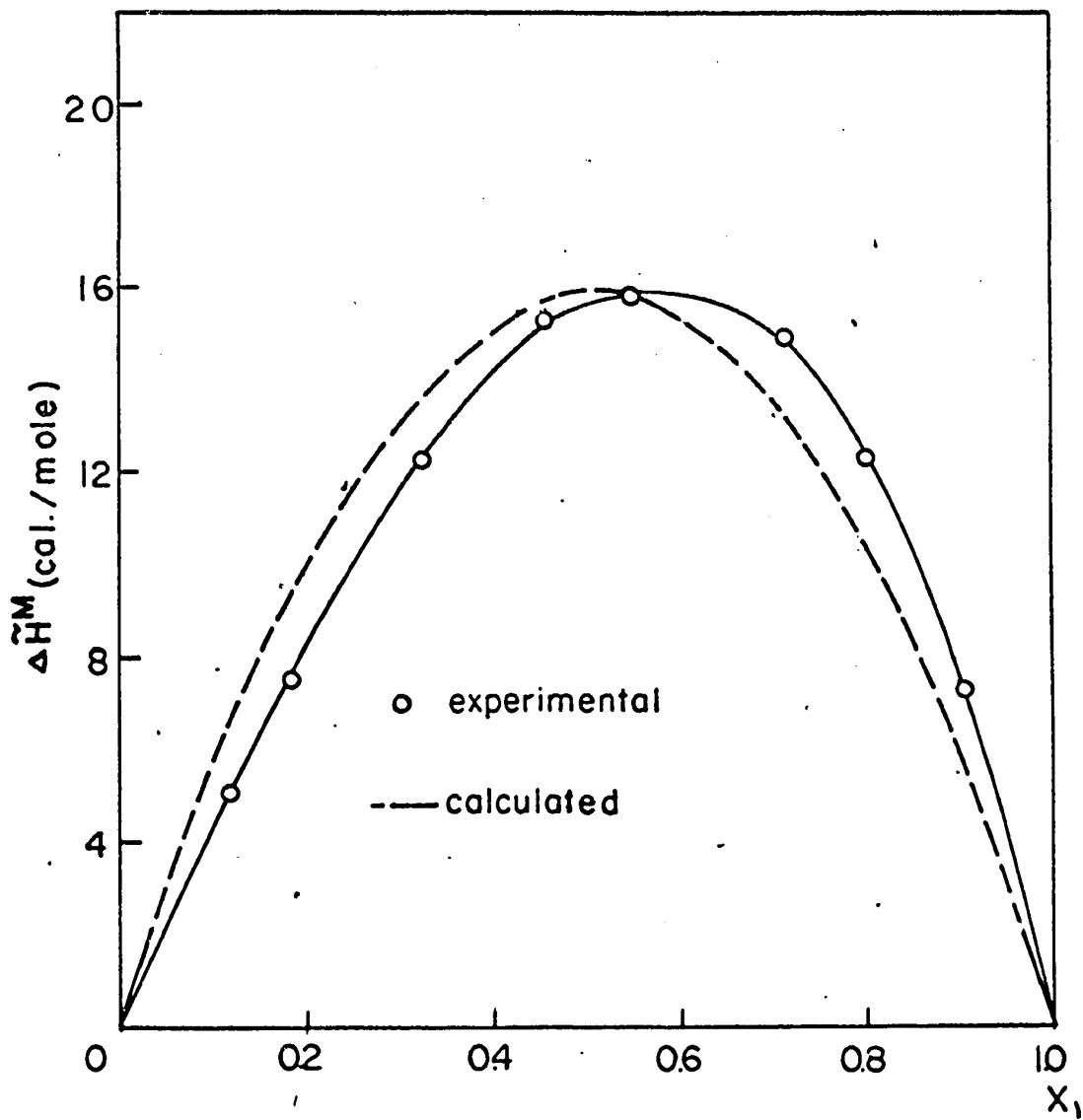


Fig.8 Heats of mixing values predicted by using solubility parameters for the system: carbontetrachloride-tetrachloroethylene.

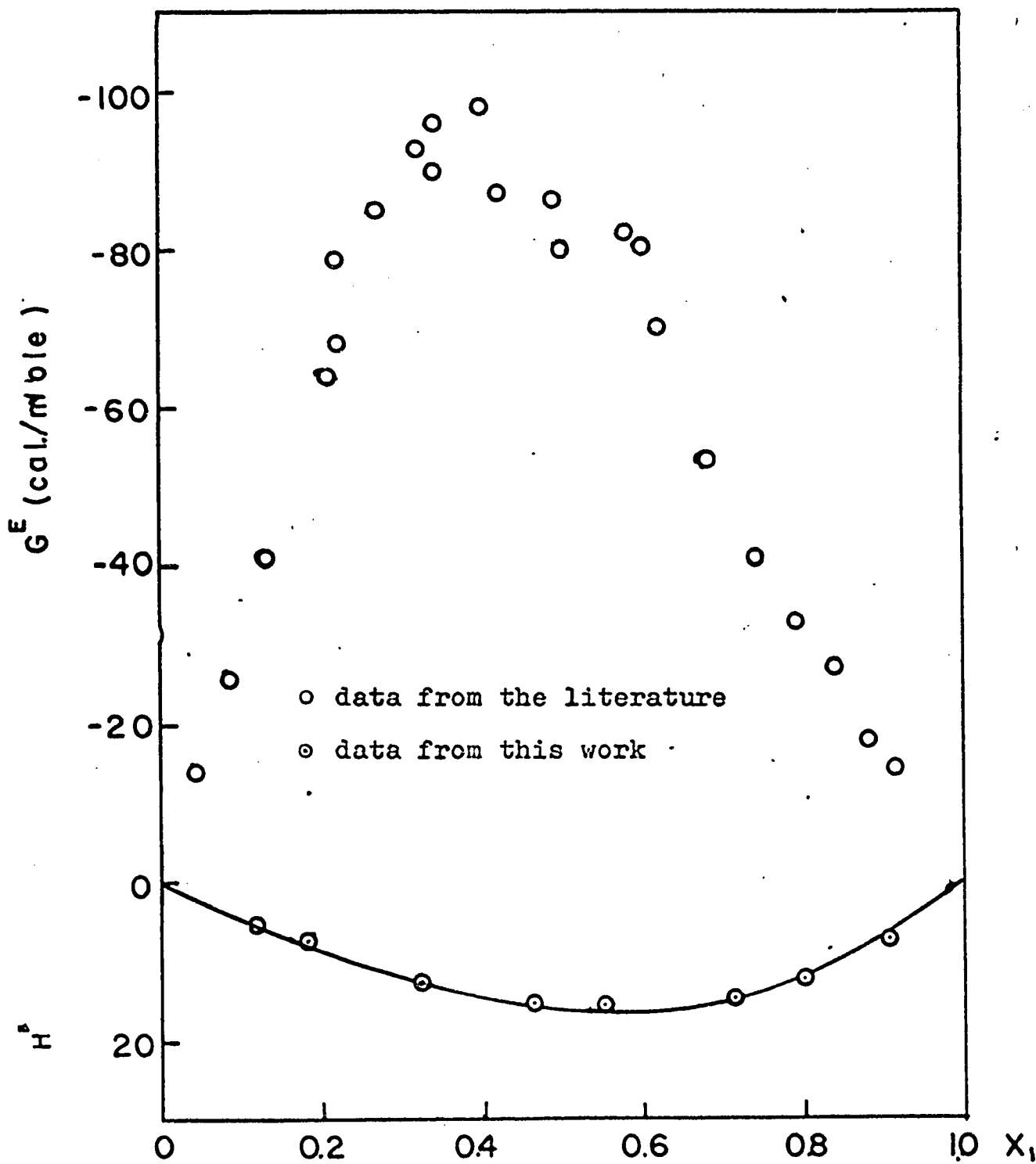


Fig.29 A comparison of the excess free energy of mixing with the excess enthalpy of mixing for carbon tetrachloride- tetrachloroethylene, at 25° C.

PART II

LIQUID PHASE ADSORPTION

INTRODUCTION

In interpreting the thermodynamic properties of real systems it is convenient to establish an "ideal" or "perfect" reference behaviour; deviations from perfect behaviour are then described in terms either of activity coefficients or of the closely related excess functions. For the studies of liquid phase adsorption, if a simple molecular model is taken as a reference system, then a study of deviations from it can lead to a clearer understanding of the real system.

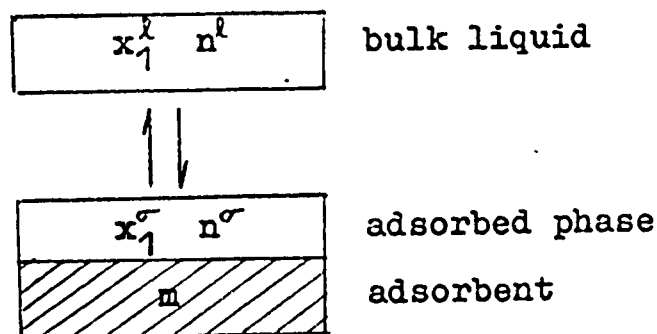
For liquid phase adsorption, so far the measuring of activity coefficients in adsorbed liquid phases is still in a preliminary stage, and few suitable data are available for analysis. A consistent theoretical basis for the study of adsorption from solutions has been developed by Everett⁽⁴⁾. Lu and Lama⁽³³⁾ made a study on the system benzene-cyclohexane-silica gel. Basing on the model of a perfect solution in contact with a Langmuir-type adsorbing surface as proposed by Everett⁽⁴⁾, deviations were described by evaluating the activity coefficients of the components in the adsorbed phase. Separation factor K' was evaluated, with con-

sideration of deviations in both the bulk liquid phase and the adsorbed phase.

For the system which Lu and Lama has studied, both benzene and cyclohexane are of approximately the same molecular size, such that the modes of being adsorbed to the surface are similar. With chain molecules such as n-hexane, n-heptane, n-octane and n-decane, the modes of being adsorbed to surfaces would be different from one another and would be different from benzene. Therefore an investigation on other systems with different molecular sizes will enable us to understand more about the adsorbed phase, and also provides a good means for testing the physical model and theoretical interpretation Lu and Lama have adopted. The systems benzene-n hexane-silica gel, benzene-n heptane-silica gel, benzene-n octane-silica gel and benzene-n decane-silica gel are chosen for this investigation. Benzene serves as a solvent, and the solutes are of different chain length; and all these n-alkanes are of different molecular size from benzene, which is aromatic. It is expected that this investigation will enable us to know more about the effect of chain length, as well as molecular shape, when molecules are adsorbed to surfaces.

LITERATURE SURVEY

When liquid phase adsorption occurs on the surface of a solid adsorbent, we consider the equilibrium between the bulk liquid phase and the adsorbed phase,



where, there is n^σ moles of solution in the adsorbed phase and n^l moles of solution in the liquid phase. The mole fraction of component 1 at the liquid phase is x_1^l and the mole fraction of component 1 at the adsorbed phase is x_1^σ ; and the adsorption occurs on m grams of adsorbent. If we start with n^o moles of solution of composition x_1^o, x_2^o , and end up with an equilibrium situation, then

$$n^o = n^l + n^\sigma \tag{10a}$$

From a material balance of component 1,

$$n^o x_1^o = n^\sigma x_1^\sigma + n^l x_1^l \quad (10b)$$

Combining (10a) and (10b),

$$\frac{n^o (x_1^o - x_1^l)}{m} = \frac{n^\sigma}{m} (x_1^\sigma - x_1^l) \quad (11)$$

Kipling⁽¹⁹⁾ and others^{(4), (20)} showed that the change of concentration of the bulk liquid due to adsorption, $(x_1^o - x_1^l)$ was directly proportional to the Gibbs adsorption, e.i. the excess of a given substance in the bulk of the mixture.

The magnitude of the Gibbs adsorption depends on how the concentration in the mixture is expressed, and on the portion of mixture on the surface of the adsorbent and in the bulk being compared.

If they are compared with respect to the number of moles,

$$x_1^{(N)} = \frac{n^o (x_1^o - x_1^l)}{m} \quad (12)$$

If they are compared by weight,

$$x_1^{(G)} = \frac{W^{\circ} (r_1^{\circ} - r_1^{\ell})}{m M_1} \quad (13)$$

If they are compared by volume,

$$x_1^{(V)} = \frac{V^{\circ} (\phi_1^{\circ} - \phi_1^{\ell})}{m V_1} \quad (14)$$

where,

W° is the weight of the initial mixture

r_1° is the weight fraction of the initial mixture

r_1^{ℓ} is the weight fraction of the equilibrium mixture

M_1 is the molecular weight of component 1.

V° is the volume of the initial mixture

ϕ_1° is the volume fraction of the initial mixture

ϕ_1^{ℓ} is the volume fraction of the equilibrium mixture

V_1 is the molar volume of component 1

Since adsorbents differ in their surface area Σ_s , it is important to obtain the absolute magnitude of the adsorption, that is,

$$\Gamma_1^{(N)} = \frac{x_1^{(N)}}{\Sigma_s} \quad (15)$$

$$p_i^{(G)} = \frac{x_1^{(G)}}{\sum_s} \quad (16)$$

$$p_i^{(V)} = \frac{x_1^{(V)}}{\sum_s} \quad (17)$$

where $\sum_i p_i^{(N)} = \sum_i p_i^{(G)} M_i = \sum_i p_i^{(V)} v_i \quad (18)$

Kiselev⁽¹²⁾ studied the adsorption from mixtures of benzene-n-heptane on silica adsorbents. It was found that the specific surface of the adsorbent determined by liquid adsorption did not always agree with those data obtained from nitrogen adsorption. Kiselev also found that a reduction in pore diameter caused an increase in the adsorption of benzene per unit surface area ^{and pore} confirmed by Jones and Stuart⁽²³⁾ through measurements on the system benzene-cyclohexane with silica gel.

Kiselev⁽²²⁾ also showed that a decrease in the pore size in silica gels caused an increase in the adsorption of benzene and n-heptane vapor at low surface coverage.

Kiselev and Pavlova⁽²⁴⁾ studied the effect of surface hydration of silica gels on the adsorption of benzene-n-heptane mixtures. It was found that with hydrated silica gels the adsorption of benzene from solution in n-hexane was better than the adsorption on dehydrated gels.

Jones and Stuart⁽²³⁾ and Kiselev⁽²⁴⁾ studied the effect of temperature on adsorption from solutions, on silicas. It was found that the adsorption decreased with a rise in temperature.

On binary liquid mixture adsorptions Bartell and Sloan⁽²⁵⁾ assumed that the individual adsorption isotherms of both components follow a Freundlich equation:

$$\frac{n_1^g}{m} = k_1 (x_1^l)^\alpha \quad (19)$$

$$\frac{n_2^g}{m} = k_2 (x_2^l)^\beta \quad (20)$$

so as to resolve the composite adsorption isotherm, which showed the separate adsorption of each component. n_1 and n_2 are the number of moles of components 1 and 2 respectively, adsorbed on m grams of adsorbent; and k_1, k_2, α, β are constants.

With this assumption, an expression for the isotherm of concentration change was obtained:

$$\frac{n^{\circ} (x_1^{\circ} - x_1^l)}{m} = k_1 (x_1^l)^{\alpha} (1 - x_1^l) - k_2 (x_1^l)^{\beta} (1 - x_1^l) \quad (21)$$

Kipling and Tester⁽²⁶⁾ reached an expression:

$$\frac{n^{\circ} (x_1^{\circ} - x_1^l)}{m} = \frac{K_3 k_3 x_1^l (1 - x_1^l)}{1 + k_3 x_1^l} - \frac{K_4 k_4 x_1^l (1 - x_1^l)}{1 + k_4 (1 - x_1^l)} \quad (22)$$

with the assumption that the individual adsorption isotherms followed a Langmuir equation:

$$\frac{n_1^{\sigma}}{m} = K_3 \frac{k_3 x_1^l}{1 + k_3 x_1^l} \quad (23)$$

$$\frac{n_2^{\sigma}}{m} = K_4 \frac{k_4 x_1^l}{1 + k_4 x_1^l} \quad (24)$$

where K_3 , K_4 , k_3 and k_4 were constants.

It was reported⁽²⁶⁾ that the individual isotherms

calculated from equations (21) and (22) revealed a wide discrepancy.

Elton⁽²⁷⁾ and Kipling⁽²⁶⁾ came up to the expression

$$x_1^\sigma = \frac{x_1^l + \frac{\Phi_2}{\Sigma_s} x_1^{(N)}}{1 + \frac{\Phi_2 - \Phi_1}{\Sigma_s} x_1^{(N)}} \quad (25)$$

This was based on the postulation that the surface of the solid adsorbent was completely covered by a monolayer in adsorption from binary liquid mixtures, where

$$\Sigma_s = \frac{n_1^\sigma}{m} \Phi_1 + \frac{n_2^\sigma}{m} \Phi_2 \quad (26)$$

Φ_1 and Φ_2 were the areas occupied per mole of components 1 and 2 respectively, if they were adsorbed separately. Σ_s was the surface area of 1 gram of adsorbent. Equation (25) was resulted by solving equations (11) and (26).

Schiessler and Rowe⁽²⁸⁾ gave a discussion of the adsorption isotherms from binary liquid mixtures. The discussion was based on the concept of constant relative adsorbability expressed in volumes.

$$K(V) = \frac{\phi_1^\sigma \phi_2^\ell}{\phi_2^\sigma \phi_1^\ell} \quad (27)$$

A material balance of component 1 together with equation (27) gave

$$\phi_1^\ell = \frac{\phi_1^\ell \phi_2^\ell}{x_1(V)} \left(\frac{1}{K(V) - 1} \right) + V^\sigma \quad (28)$$

where V^σ was the adsorptive capacity in cc/gm. Plots of $(\phi_1 \phi_2)^\ell / x_1(V)$ against ϕ_1^ℓ resulted in straight lines and V^σ and $K(V)$ could be determined.

Siskova and Erdos⁽²⁹⁾ combined the expression for the separation factor expressed in moles, namely

$$K(N) = \frac{x_1^\sigma}{x_2^\sigma} \frac{x_2^\ell}{x_1^\ell} \quad (29)$$

equation (29) with equation (3) yield

$$\frac{x_1^{(N)}}{1-x_1^\ell} = -\frac{1}{K^{(N)}} \frac{x_1^{(N)}}{x_1^\ell} + \frac{n^\sigma}{m} \left(\frac{K^{(N)} - 1}{K^{(N)}} \right) \quad (30)$$

plots of $x_1^{(N)} / (1-x_1^\ell)$ against $x_1^{(N)} / x_1^\ell$ resulted in straight lines from which n^σ/m and $K^{(N)}$ was determined.

Cleland⁽³⁰⁾ studied the adsorption of mixtures of benzene with cyclohexane, benzene with carbontetrachloride, and carbontetrachloride with cyclohexane, on porous (Vycor) glass. He used his own data and some data from others and found good agreement between the separation factor $K^{(N)}$ for silica gel and for Vycor glass adsorbents. But these two substances had different molar area from nitrogen adsorption calculations. It was found to be $230 \cdot 10^3 \text{ m}^2/\text{mole}$ for silica gel and $430 \cdot 10^3 \text{ m}^2/\text{mole}$ for Vycor glass.

Everett⁽⁴⁾ proposed an equation similar in form to Equation (30), but expressed in terms of moles, which he used to calculate the adsorptive capacity $N^\sigma (=n^\sigma/m)$ and the separation factor $K^{(N)}$. This will be discussed again in the following section.

THEORETICAL CONSIDERATIONS

Basing on the assumptions: (1) monomolecular adsorption; (2) perfect solution-solid interface; (3) all adsorption sites have identical properties, Everett⁽⁴⁾ derived an equation:

$$\frac{x_1^l x_2^l}{\left(\frac{n^o \Delta x_1^l}{m} \right)} = \frac{m}{n^\sigma} \left(x_1^l + \frac{1}{K - 1} \right) \quad (31)$$

where x_1^l, x_2^l are the mole fractions of component 1 and 2 respectively, of the equilibrium solution;

n^o is the number of moles of solution before adsorption;

Δx_1^l is equal to $x_1^\sigma - x_1^l$ by definition; and x_1^o is the mole fraction of component 1 of the original solution;

m is the weight of adsorbent in grams;

n^σ is the number of moles of solution in the adsorbed phase;

K is the separation factor.

If $x_1^l x_2^l / (n^\sigma \frac{x_1^l}{m})$ is plotted against x_1^l , a straight line would be obtained. The intercept of the straight line will give $\frac{m}{n^\sigma} (\frac{1}{K-1})$ and the slope will give m/n^σ . By solving two simultaneous equations, n^σ and K can be evaluated.

In interpreting the thermodynamic properties of real systems it is convenient to establish an ideal reference behavior; deviations from ideal behavior are then described in terms of activity coefficient or of the closely related excess functions.

Equation (31) governs an ideal model, therefore it is desirable to evaluate the deviations so that real systems can be described. Everett⁽³¹⁾ derived an expression for equilibrium liquid phase adsorption:

$$\ln \gamma_2^\sigma = x_1^\sigma \ln \left(\frac{x_1^\sigma x_2^l \gamma_2^l}{x_2^\sigma x_1^l \gamma_1^l} \right) - \int_0^{x_1^\sigma} \ln \left(\frac{x_1^\sigma x_2^l \gamma_2^l}{x_2^\sigma x_1^l \gamma_1^l} \right) dx_1^\sigma \quad (32a)$$

$$\ln \gamma_1^\sigma = x_2^\sigma \ln \left(\frac{x_2^\sigma x_1^l \gamma_1^l}{x_1^\sigma x_2^l \gamma_2^l} \right) - \int_0^{x_2^\sigma} \ln \left(\frac{x_2^\sigma x_1^l \gamma_1^l}{x_1^\sigma x_2^l \gamma_2^l} \right) dx_2^\sigma \quad (32b)$$

where σ denotes adsorbed phase and l denotes liquid phase.

Therefore the activity coefficients of the components in the adsorbed phase can be evaluated, provided

the data for the necessary terms are available.

The compositions in the adsorbed phase can be evaluated in terms of x_1^l , n^o and n^σ , by the expression:

$$x_1^\sigma = x_1^l + \Delta x_1^l \left(\frac{n^o}{n^\sigma} \right) \quad (33)$$

To derive Equation (33), we define

$$\Delta x_1^l = x_1^o - x_1^l \quad (34)$$

$$\text{then, } \Delta x_1^l = \frac{n_1^o}{n^o} - \frac{n_1^o - n_1^\sigma}{n^l}$$

$$= \frac{n_1^o n^l - n_1^o n^o + n_1^\sigma n^o}{n^o n^l}$$

$$= \frac{n_1^o n^l - n^o (n_1^o - n_1^\sigma)}{n^o n^l}$$

$$= \frac{n_1^o n^l - n_1^\sigma n^l}{n^o n^\sigma} \frac{n^\sigma}{n^l}$$

$$= \frac{(n_1^\sigma + n_1^l) n^l - (n^\sigma + n^l) n_1^l}{n^o n^\sigma} \frac{n^\sigma}{n^l}$$

$$= \frac{n_1^\sigma n^l - n_1^l n^\sigma}{n^\sigma n^l} \frac{n^\sigma}{n^o}$$

$$= \left(\frac{n_1^\sigma}{n^\sigma} - \frac{n_1^l}{n^l} \right) \frac{n^\sigma}{n^0}$$

$$= \left(x_1^\sigma - x_1^l \right) \frac{n^\sigma}{n^0}$$

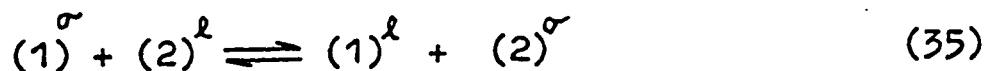
rearranging,
$$x_1^\sigma = x_1^l + \Delta x_1^l \left(\frac{n^0}{n^\sigma} \right) \quad (33)$$

The liquid solutions under investigation were not ideal ones. The deviations from an ideal model can be expressed in terms of activity coefficients. These activity coefficients at the required conditions cannot be obtained in literature, therefore Lu's method⁽³²⁾ of extrapolating activity coefficients in liquid phase was adopted. It was shown that over a moderate temperature range the relative partial molal heat of solution at a constant liquid composition varies linearly with temperature, and the logarithm of the liquid coefficient, $\ln \gamma^l$, at a given composition should involve three temperature terms of the form $a + b/T + c \ln T$. Hence if the available data of $\ln \gamma^l$ are not given at the desired conditions, extrapolation can be performed to obtain γ^l by using three sets of vapor-liquid equilibrium data, or by using two sets of vapor-liquid equilibrium

data together with values of heats of mixing of the liquid components. It was found (33) that for the system benzene-cyclohexane at 25° C, same values were obtained when extrapolated: (1) with 2 sets of heats of mixing data and 1 set of vapor-liquid equilibrium data: (2) with 1 set of heats of mixing data and 2 sets of vapor-liquid equilibrium data.

Once the compositions x_1^σ and x_2^σ in the adsorbed phase are evaluated, the separation factor, K, can be corrected for a real system by considering deviations from the ideal one estimated by equation (37).

If simple chemical equilibrium principles are intuitively applied to the phase-exchange reaction,



where (1) and (2) denote concentrations of components 1 and 2 respectively; and σ , l denote the adsorbed phase and liquid phase. The equilibrium constant will be

$$K = \frac{x_1^\sigma x_2^l}{x_1^l x_2^\sigma} \quad (36)$$

This expression of K has the same form as the

" separation factor " in the vapor-liquid equilibrium of a perfect solution:

$$k = \frac{x_1^g x_2^l}{x_1^l x_2^g}$$

and therefore the K of equation (36) is also denoted as a separation factor.

In discussion of physico-chemical equilibrium, activity coefficients are often introduced as quantities by which individual concentration terms have to be multiplied to maintain the validity of the law of mass action. On this basis we might write down the general form of equation (36), for equilibrium between components 1 and 2 in the liquid l and adsorbed σ phases,

$$K' = \frac{x_1^\sigma \gamma_1^\sigma x_2^l \gamma_2^l}{x_1^l \gamma_1^l x_2^\sigma \gamma_2^\sigma} \quad (37)$$

Hence K' in equation (37) is the corrected separation factor for real systems while the K in equation (36) is the separation factor for perfect systems only.

Applying Gibbs Duhem equation to the adsorbed phase,

$$x_1^\sigma d \ln \gamma_1^\sigma + x_2^\sigma d \ln \gamma_2^\sigma = 0$$

Handwritten note: $\gamma_2^\sigma d \ln \gamma_1^\sigma = \gamma_1^\sigma d \ln \frac{\gamma_2^\sigma}{\gamma_1^\sigma}$

integrating, $\ln \gamma_2^\sigma = \int x_1^\sigma d \ln \left(\frac{\gamma_2^\sigma}{\gamma_1^\sigma} \right) + \text{constant}$

integrating by parts and setting the lower limit of the integration to $x_1^\sigma = 0$, we have

$$\ln \gamma_2^\sigma = x_1^\sigma \ln \left(\frac{\gamma_2^\sigma}{\gamma_1^\sigma} \right) - \int_0^{x_1^\sigma} \ln \left(\frac{\gamma_2^\sigma}{\gamma_1^\sigma} \right) dx_1^\sigma \quad (37a)$$

in particular, integrating from $x_1^\sigma = 0$ to $x_1^\sigma = 1$,

$$\int_0^1 \ln \left(\frac{\gamma_2^\sigma}{\gamma_1^\sigma} \right) dx_1^\sigma = 0 \quad (37b)$$

multiply the logarithm of eq.(37) by dx_1^σ and integrate,

$$\int_0^{x_1^\sigma} \ln \left(\frac{x_1^\sigma x_2^\ell \gamma_2^\ell}{x_2^\sigma x_1^\ell \gamma_1^\ell} \right) dx_1^\sigma = \int_0^{x_1^\sigma} \ln \left(\frac{\gamma_2^\sigma}{\gamma_1^\sigma} \right) dx_1^\sigma + x_1^\sigma \ln K' \quad (37c)$$

substituting eq.(37b) into eq.(37c),

$$\ln K' = \int_0^1 \ln \left(\frac{x_1^\sigma x_2^\ell \gamma_2^\ell}{x_2^\sigma x_1^\ell \gamma_1^\ell} \right) dx_1^\sigma \quad (37d)$$

This provides a convenient way to calculate K' .

EXPERIMENTAL DETAILS

MATERIALS

Gases

The nitrogen was of the "dry" grade with a minimum purity of 99.99%; the helium conformed to the specifications of the U.S. Bureau of Mines for grade "A" helium, the purity of which was 99.995%. They were passed through a column packed with activated silica gel in order to remove traces of water.

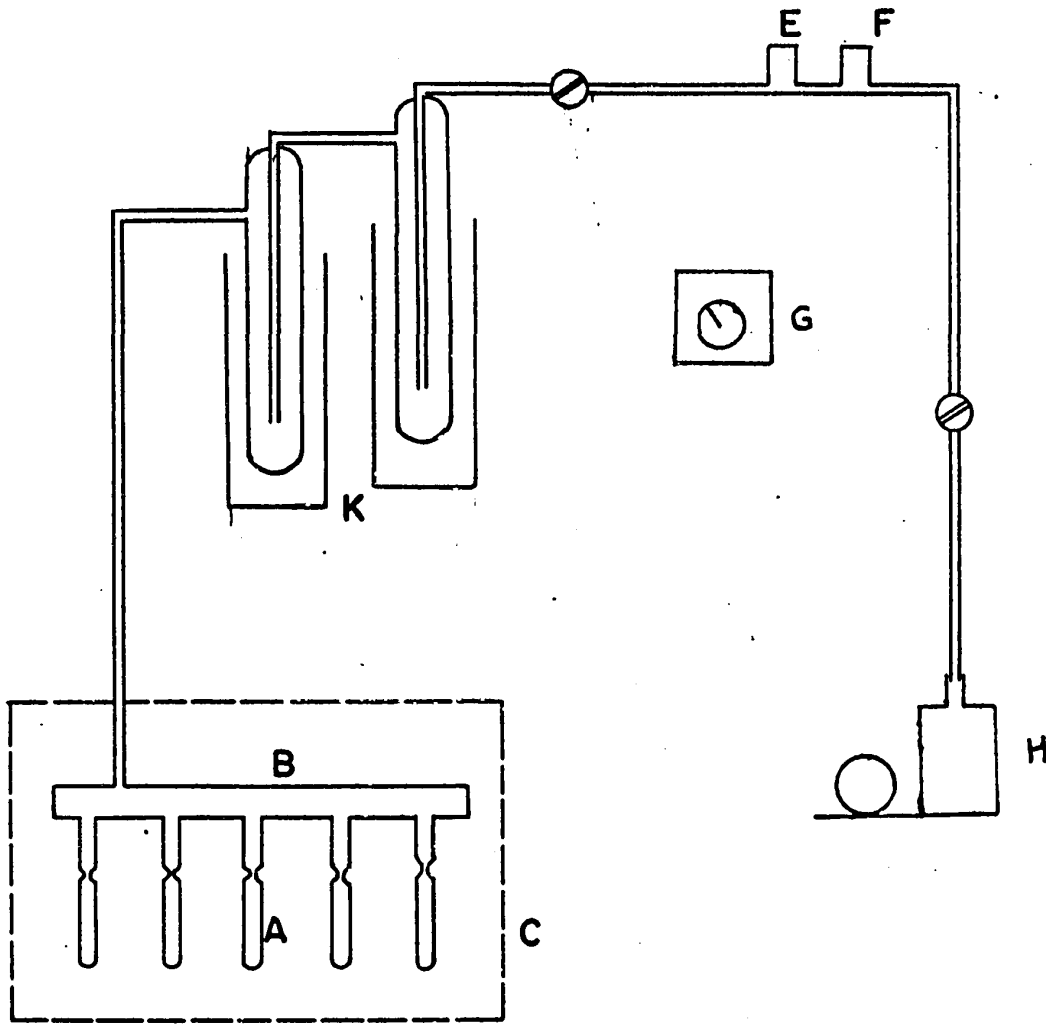
Adsorbent

The adsorbent was prepared from a commercial silica gel (20-200 mesh, Davison) obtained from Fisher Scientific Co. Samples of 20 to 50 grams of adsorbent were digested with nitric acid⁽³⁴⁾ 1 : 1 by volume, followed by an extraction with nitric acid 1:10 and then with four litres of distilled water per gram of sample. During the washing, which was done in a Buchner funnel, the adsorbent was always kept under water. Washing was followed by drying in an oven at 140° C for 24 hours.

Following this treatment, the very fine particles

were separated by sedimentation of the samples in 900 cc of distilled water, using a one-litre graduated cylinder sitting vertically. The portion of the sample remaining in suspension after one minute was discarded; the residue was dried in the oven at 140° C.

Thermal degassing of the samples at reduced pressures was performed. The apparatus for this purpose was shown schematically in Fig.9. The apparatus consisted of glass ampoules (A) containing the adsorbent, a glass manifold (B) in the vacuum line, a temperature-controlled oven (C), two traps cooled by liquid nitrogen (K), a Pirani head (E), a Penning head (F), a Pirani-Penning type vacuum gauge (G), a vacuum pump (H) and suitable connections. The traps served two purposes, namely, (1) condensing the water vapor resulting from the degassing of the adsorbent; and (2) trapping particles of the adsorbent blown off the glass ampoules during evacuation. Portions of approximately 3 grams of adsorbent were placed in pyrex-glass ampoules, which were then joined onto the glass manifold mounted inside the temperature-controlled oven. The adsorbent was degassed for at least 40 hours at 140° C and at a pressure of 3×10^{-5} mm Hg, after which period the ampoules were then stored in a desiccator with activated silica gel.



- | | | | |
|---|----------------|---|-----------------------------|
| A | GLASS AMPOULES | E | PIRANI HEAD |
| B | GLASS MANIFOLD | F | PENNING HEAD |
| C | OVEN | G | PIRANI-PENNING VACUUM GAUGE |
| K | COLD TRAPS | H | VACUUM PUMP |

Fig.9 The degassing oven

Liquids

The liquids used in this study are listed in Table (3), together with their grade and purity. A comparison of measured and literature values of their refractive indices at 25° C is also described. The hydrocarbons were dehydrated in the following procedures: about 3 grams of activated silica gel was added to a flask containing 50 cc of a pure hydrocarbon, stirred vigorously for about 2 minutes, and then the liquid was decanted into another flask; the process being repeated 3 times. The hydrocarbon was transferred into a dry 50 cc brass storage vessel, which was then centrifuged for about 10 minutes, at 10,000 R.P.M., in order to separate the solid particles in suspension. Finally, the storage vessel was stored in a desiccator with activated silica gel.

Preparation of binary mixtures

The preparation of a binary mixture was performed in a dry box under a helium atmosphere. The dehydrated reagents were taken out of the storage vessel by using a hypodermic syringe and were discharged into a 25 cc volumetric flask. The amount of each component which had been used to make up the mixture was obtained from .

Table 3

PHYSICAL PROPERTIES OF PURE LIQUIDS

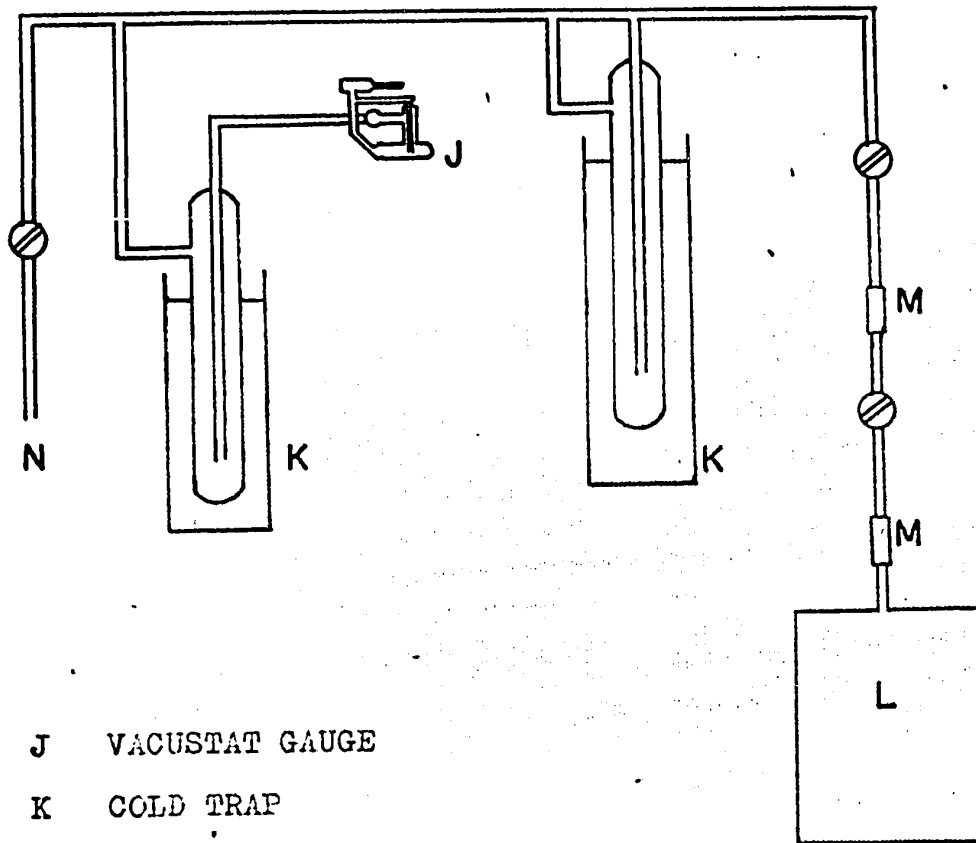
<u>Compound</u>	<u>Grade</u>	Minimum* purity <u>(mole %)</u>	Refractive index (25° C)	
			<u>Expt.</u>	<u>Lit.</u> ⁽¹⁸⁾
n-hexane	Research	99.9	1.37232	1.37226
n-heptane	Research	99.9	1.38528	1.38517
n-octane	Pure	99	1.39540	1.39505
n-decane	Pure	99	1.40972	1.40967
benzene	Spectro- grade	99	1.49783	1.49790

* Supplier's data

weighing. After both components were loaded into the flask, the flask was gently shaken for 2 minutes to ensure complete mixing. The mixture was ready for the loading of an adsorption vessel. It was important that the mixture was made up shortly before loading the adsorption vessel to minimize the change of composition due to evaporation.

Loading the adsorption vessel

The structure of an adsorption vessel was the same as that of a mixing vessel as shown in fig.1, except that no tin-foil was necessary for separating the two compartments. A dry adsorption vessel was first weighed and then was put in a brass desiccator, which was connected to a vacuum system to be evacuated to 10^{-3} mm Hg. The brass desiccator was shown schematically in fig.10, together with the vacuum system. When the vacuum in the system reached 10^{-3} mm Hg read from a vacustat gauge, the valve on the desiccator was closed and the desiccator together with the adsorption vessel inside were put in the dry box. Inside the dry box, an ampoule of silica gel and a prepared binary liquid mixture were ready for loading. Under the helium atmosphere, the desiccator was opened. The ampoule was



- J VACUSTAT GAUGE
- K COLD TRAP
- L BRASS DESICCATOR
- M RUBBER SLEEVES
- N TO VACUUM PUMP

Fig.10 The brass desiccator

broken and the silica gel was transferred to the adsorption vessel. The plugs were tightly closed. The dry box was opened and the vessel was weighed again so as to obtain the weight of the silica gel which had been put into the vessel. The vessel was put in the brass desiccator again, which was evacuated to 10^{-3} mm Hg. The desiccator and the vessel were re-opened in the dry box under a helium atmosphere, and the vessel was loaded with the prepared binary liquid mixture. The plugs were re-closed and the excess liquid was blown off with a stream of helium gas. The dry box was opened and the vessel was weighed again so as to obtain the amount of liquid mixture used.

Equilibrium adsorption

The vessel was put in the brass jacket as shown in Fig. 2, and the jacket was immersed into the water bath at $25 \pm 0.005^\circ \text{C}$ as described on page 14. No evacuation was performed because it was not necessary. At least 4 hours were allowed for equilibrium adsorption and the vessel was vigorously shaken every half an hour to ensure good mixing of the contents.

Analysis of the equilibrium liquid mixture

After 4 hours, the mixing vessel was taken out and centrifuged for 5 minutes at 10,000 R.P.M., to separate the solid particles in suspension. The liquid composition was analysed by a Precision Refractometer. The refractometer was a Bauch and Lomb Abbe-3 type, capable of determining values to 0.00001. The accuracy of readings was of the order of 0.00003. A precision temperature controller was used to keep the temperature of the instrument at 25 ± 0.02 C. The refractometer was located in a room where the temperature was controlled at 25 ± 0.5 C.

Calibration curves of the refractive indices for the systems under investigation was obtainable in the literature⁽³⁵⁾. A few checking runs showed that experimental data agreed very well with the literature ones, as shown in fig.28. The values from the literature are listed in Tables 3 and 4.

Surface area of silica gel

The measurement of the surface area of the silica gel was performed with a B.E.T. gravimetric apparatus, schematically shown in fig. 11. A light quartz bucket

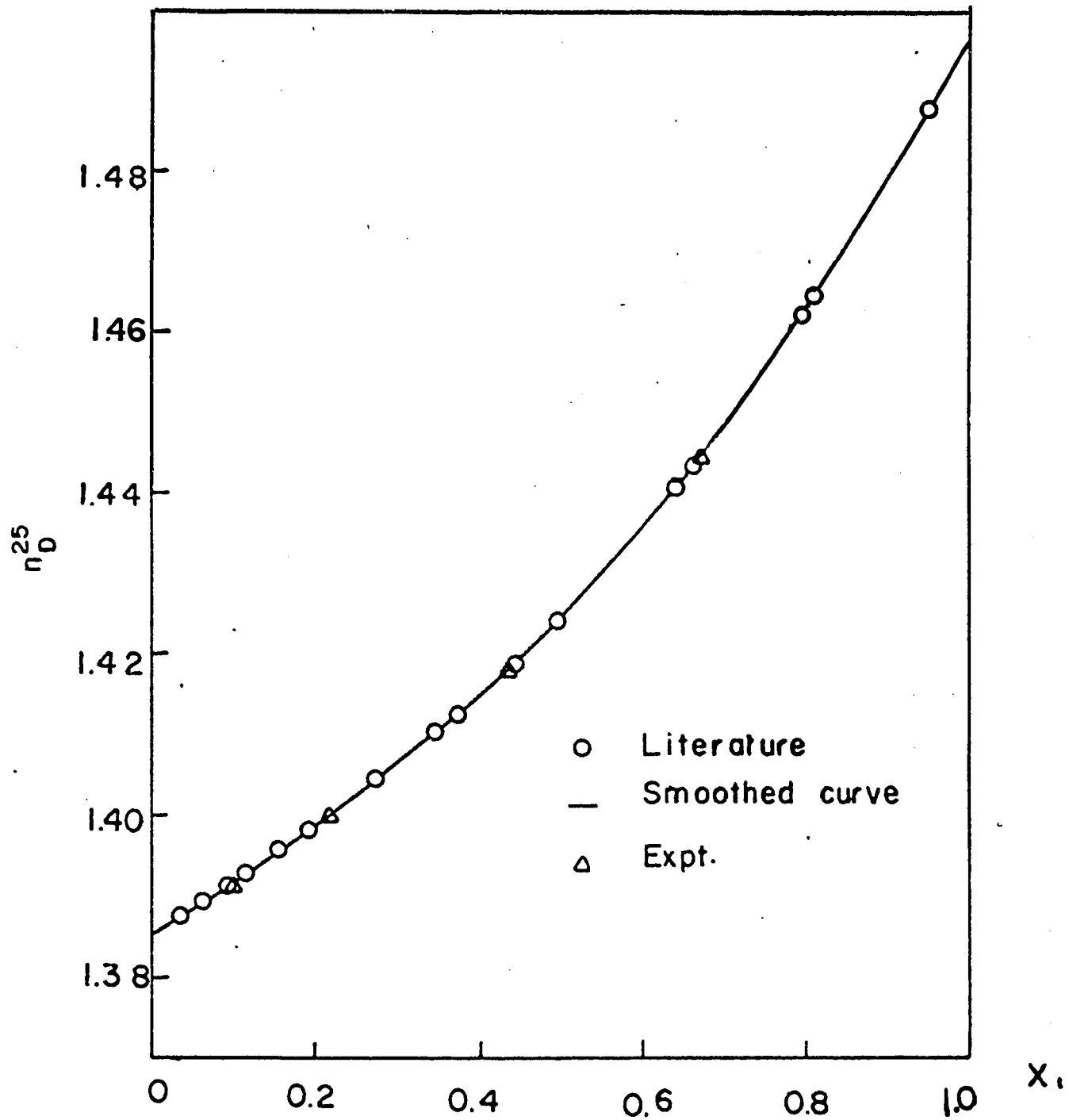


fig.28 Calibration curve on refractive indices for the system benzene-n-heptane at 25°C

Table 4a

CALIBRATION DATA ON REFRACTIVE INDICES (35)

benzene(1)-n hexane(2)		benzene(1)-n heptane(2)	
x_1	$n_D^{25^\circ}$	x_1	$n_D^{25^\circ}$
0.0245	1.37423	0.0366	1.38750
0.0663	1.37765	0.0632	1.38918
0.1616	1.38581	0.0925	1.39109
0.1943	1.38878	0.1193	1.39288
0.3386	1.40272	0.1920	1.39799
0.4894	1.41935	0.3452	1.41014
0.6482	1.43954	0.4932	1.42400
0.7936	1.46090	0.6420	1.44061
0.9500	1.48821	0.7994	1.46214
		0.9501	1.48789
		0.1012*	1.39183*
		0.2213*	1.40046*
		0.4337*	1.41788*
		0.6750*	1.44498*

* experimental data by the author

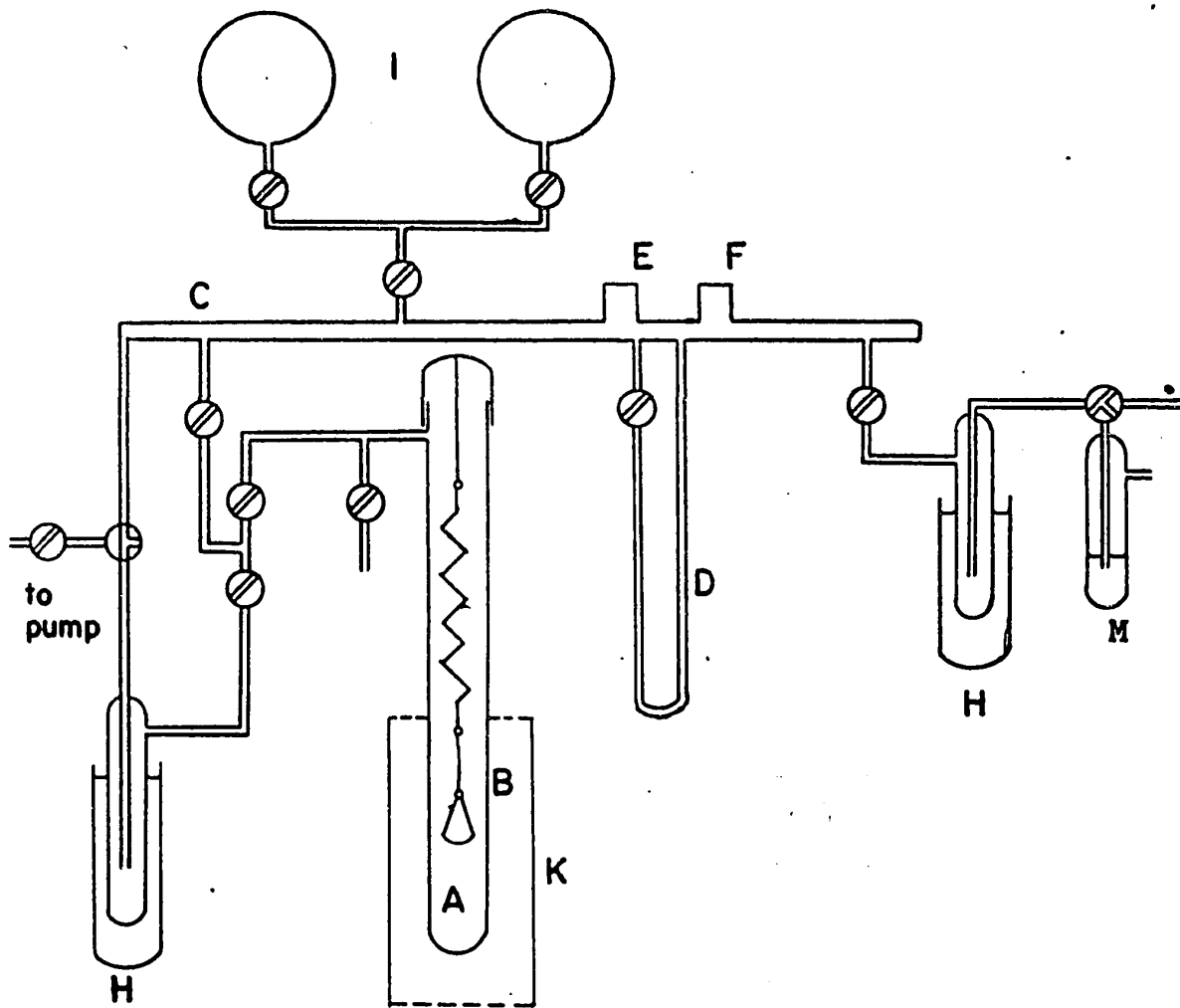
Table 4b

CALIBRATION DATA ON REFRACTIVE INDICES (35)

benzene(1)-n octane(2)		benzene(1)-n decane	
x_1	$n_D^{25^\circ}$	x_1	$n_D^{25^\circ}$
0.0294	1.39676	0.0384	1.41105
0.0531	1.39796	0.0648	1.41196
0.1031	1.40053	0.1698	1.41591
0.1175	1.40132	0.2426	1.41910
0.1296	1.40200	0.2527	1.41956
0.2087	1.40662	0.3683	1.42545
0.3450	1.41565	0.4232	1.42873
0.4990	1.42808	0.5000	1.43376
0.5770	1.43552	0.6059	1.44198
0.6405	1.44223	0.6461	1.44562
0.8004	1.46257	0.6995	1.45098
0.9468	1.48711	0.8305	1.46703
		0.9484	1.48684

(A) was suspended from a calibrated quartz spring, by a glass fibre. These parts were enclosed in a cylindrical Pyrex glass column (B) with an outside diameter of $1 \frac{1}{4}$ in., an overall height of 54 in., with a conical tapered joint on top, for the purpose of loading and unloading the bucket. The adsorption column was connected to a mercury manometer (D), a Penning head (E), a Pirani head (F) with a Pirani-Penning type vacuum gauge, a trap cooled by liquid nitrogen (H), two nitrogen-reservoir flasks (I), an oil diffusion pump and suitable connections and stopcocks. A movable external furnace (K) connected to a temperature controller was used to maintain isothermal conditions. Degassing temperature was measured by using an iron-constantan thermocouple placed between the heater and the external surface of the column. Potential measurements were made with a K-3 potentiometer. This McBain balance had a sensitivity of about 1 mm extension per mg., and a capacity of 400 mg. Spring extensions and mercury manometer pressure readings were readily determined to 0.01 mm by using a cathetometer. The precision of the reading was of the order of 0.05 mm. A sample of about 200 mg. was weighed in the cal-

ibrated bucket and was degassed at 140° C to an ultimate pressure of less than 10^{-4} mm Hg. The stopcock connecting the system to the vacuum pump was then closed and the furnace was removed from the column. As the column cooled down, it was immersed in liquid nitrogen to a height of about 5 inches above the bucket. The reading of the spring extension was then recorded. Next, nitrogen was admitted into the column till the pressure was of a few mm Hg, and the manometer reading and spring extension were recorded. These readings were made frequently until constancy was obtained. The time necessary for obtaining equilibrium varied from 15 to 60 minutes, depending on the pressure; and more time was required at higher pressures. Successive admissions of nitrogen were made till sufficient points for the calculation were obtained.



- | | | | |
|---|---------------------------------|---|--------------------|
| A | QUARTZ BUCKET | E | PENNINS HEAD |
| B | PYREX CONTAINER | F | PIRANI HEAD |
| C | MANIFOLD | H | COLD TRAPS |
| D | MERCURY
MANOMETER | I | NITROGEN RESERVOIR |
| M | MERCURY SEALED
GAS REGULATOR | K | FURNACE |

Fig.11 The nitrogen adsorption apparatus

The B.E.T. method⁽¹⁴⁾

The method of Brunauer, Emmett and Teller was used to evaluate the surface area of the silica gel from the nitrogen adsorption data. The expression of the B.E.T. theory in terms of mass of adsorbate is

$$\frac{p/p_0}{W^{\sigma}(1-p/p_0)} = \frac{1}{W_m C} + \frac{C-1}{W_m C} \frac{p}{p_0} \quad (39)$$

where W^{σ} , in grams, is the mass of nitrogen adsorbed at an equilibrium pressure p and temperature T ;

W_m , in grams, is the mass of nitrogen adsorbed on W grams of silica gel at monolayer coverage;

C , is a constant;

p_0 is atmospheric pressure, 760 mm Hg.

The terms W_m and C were evaluated from a plot of the left hand side of equation (39) against the relative pressure p/p_0 . The molar area of the adsorbed nitrogen at -195°C was taken as 16.2 \AA^2 ⁽³⁸⁾.

The surface area of the adsorbent, Σ_s , in $\text{m}^2/\text{gm.}$,

was expressed as:

$$\Sigma_s = \frac{97.6 \cdot 10^3 W_m}{28.016 W} = 3481 \frac{W_m}{W}$$

where 97.6 was the molar area of nitrogen in m²/mole
and 28.016 was the molecular weight of nitrogen.

Sample calculation

A sample calculation of the surface area of silica gel is presented as the following:

Calibration of the quartz spring

length of spring without weight	36.640 cm
weight added on the spring	0.2923 gm
length of spring with weight	67.045 cm
extension	30.395 cm
extension factor = $30.395/0.2924$	0.1040 cm/mg

Experimental data

degassing pressure 10^{-4} mm Hg

degassing temperature 140°C

<u>Time (min.)</u>	<u>Length of spring (cm)</u>	<u>Pressure (mm Hg)</u>
0	36.640	0
0 (gel added)	59.546	0
40	61.614	1.64
80	62.036	3.78
140	62.600	6.88
200	62.781	9.79
260	63.278	19.76
320	63.565	26.68
380	64.324	41.11

Calculations

Using equation (39),

<u>p (cm)</u>	<u>L (cm)</u>	<u>W^σ (gm)</u>	<u>p/p_o</u>	<u>1-p/p_o</u>	<u>$\frac{p/p_o}{W(1-p/p_o)}$</u>
1.64	2.068	0.1989	0.02157	0.97843	0.01108
3.78	2.490	0.2394	0.04974	0.95026	0.02186
6.88	3.054	0.2937	0.09053	0.90947	0.03389
9.79	3.235	0.3111	0.12882	0.87119	0.04753
19.76	3.732	0.3589	0.26000	0.74000	0.09790
26.68	4.019	0.3865	0.35105	0.64895	0.13997
41.11	4.778	0.4595	0.54092	0.45908	0.25644

$\frac{p/p_o}{W(1-p/p)}$ was plotted against p/p_o , as shown in fig.12.

The intercept obtained from Fig.12 was 0.314, which was $1/W_m C$; and the slope was 34.857, which was $(C-1)/W_m C$, according to equation (39).

Using the values of the intercept and the slope, C and W_m were evaluated;

$$C = 112.0096$$

$$W_m = 0.2843$$

Using the readings of the quartz spring length and the calculated extension factor, we evaluated W, the weight of silica gel used ,

$$\begin{aligned} W &= \frac{59.546 - 36.640}{0.1040} \\ &= 2.2027 \text{ gm.} \end{aligned}$$

and hence

$$\begin{aligned} \Sigma_s &= 3481 \frac{0.2843}{2.2027} \\ &= 449.29 \text{ m}^2/\text{gm.} \end{aligned}$$

which was the surface area of the silica gel under investigation.

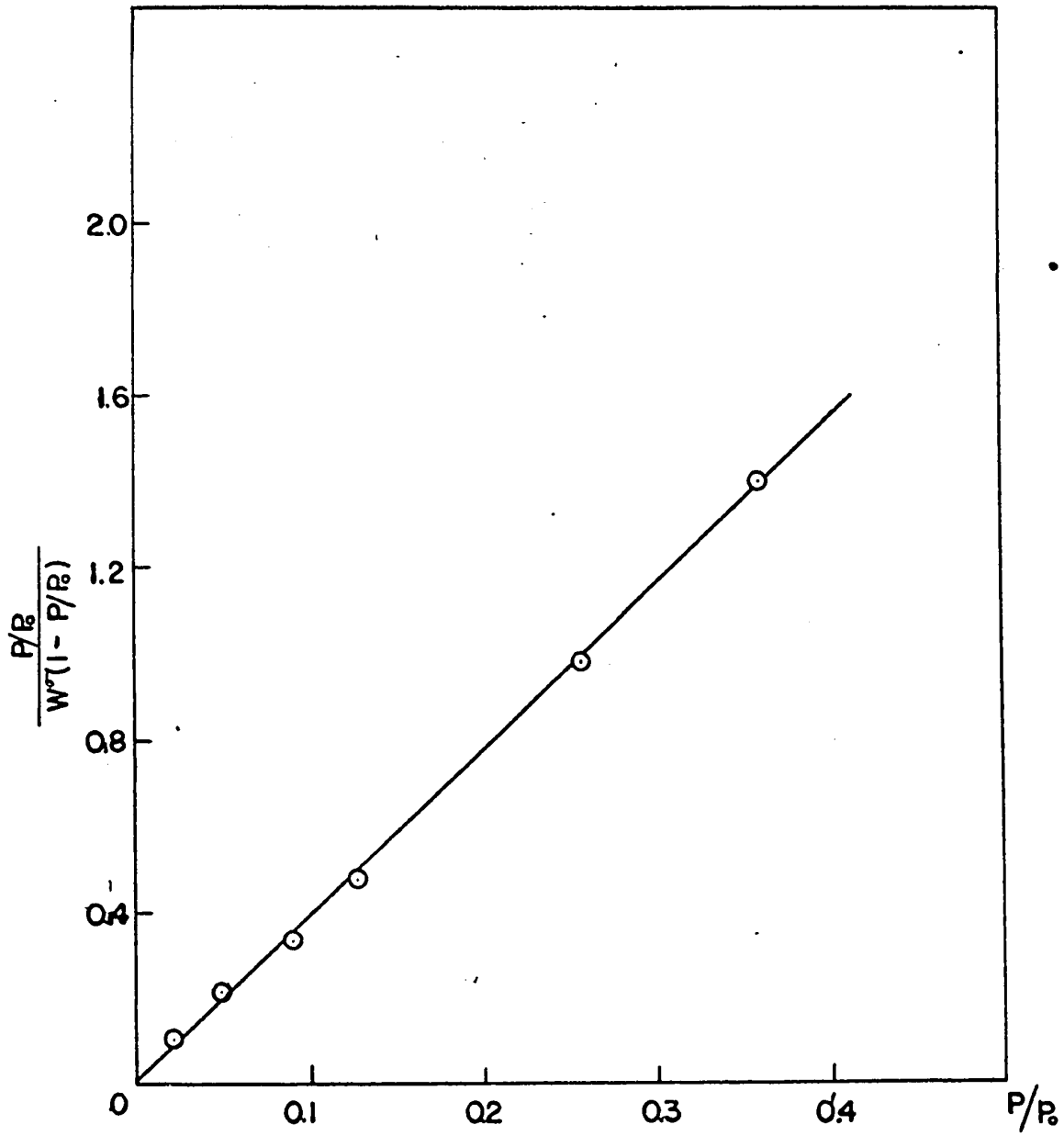


Fig.12 Surface area measurement,

a plot of $\frac{p/p_0}{W^\sigma(1-p/p_0)}$ vs p/p_0 .

PRESENTATION OF RESULTS

The compositions of the starting liquid solution were obtained from weighing. They were designated as x_1^o in Tables 5,6,7 and 8.

The amount of silica gel used in each experiment was obtained by weighing and was designated as m in Tables 5,6,7 and 8.

The amount of mixture used in each experiment was calculated and was designated as n^o in Tables 5,6,7 and 8.

Existing data were available⁽³⁵⁾ for the calibration of refractive indices for the working systems. 4 checking points were performed and good agreement was obtained, as shown in Table 4 and fig. 28. Calibration curves were prepared on large charts by using these data, as listed in Tables 4a and 4b.

The equilibrium liquid compositions were read on the calibration curves and the values were shown in Tables 5,6,7 and 8, under the column x_1^l .

Plots of $(x_1^l x_2^l) / (n^o \frac{\Delta x_1^l}{m})$ against x_1^l were made and n^o, K were evaluated as shown in fig. 13,14,15 and 16.

By using equation (33): $x_1^\sigma = x_1^l + \Delta x_1^l (n/n^\sigma)$, the compositions of the solution in the adsorbed phase, x_1^σ , were calculated and listed in Tables 5,6,7 and 8. Phase equilibrium curves are shown in fig. 17,18,19 and 20.

The liquid activity coefficients of the components were evaluated at 25°C, as shown in Appendix I; lists of the values are shown in Tables 5, 6, 7 and 8.

By using equation (32), the activity coefficients of the components at the adsorbed phase were evaluated. Results are listed in Tables 5,6 and 7; and were also shown graphically in fig. 21,22 and 23.

With enough information, the separation factor K' for real systems, were evaluated and are reported in Tables 5,6 and 7. The evaluation of the K' values was based on equation (37d).

SAMPLE CALCULATION

To illustrate the calculating procedures, the evaluation of a point for the system benzene-n-heptane-silica gel was taken as an example.

Weighings

adsorption vessel	121.6593 gm.
silica gel added	123.7720 gm.
mixture added	132.1142 gm.
<hr/>	
silica gel used	2.1127 gm.
mixture used	8.3422 gm.

Mixture preparation

bottle	23.9070 gm.
benzene added	27.7385 gm.
n-heptane added	38.6931 gm.
<hr/>	
benzene used	3.8315 gm.
n-heptane used	10.9546 gm.

Evaluation of the composition of the liquid mixture

<u>Substance</u>	<u>M.Wt.</u>	<u>gm.</u>	<u>Moles</u>	<u>x (mole fr.)</u>
benzene	78.108	3.8315	0.04905	0.3097
n-heptane	100.198	10.9546	0.10933	0.6903
		14.7861	0.15838	1.0000

molecular weight of mixture = $14.7861/0.15838$
= 93.3584 gm.

moles of mixture used = $8.3422/93.3584 = 0.08936$ moles

n_D^{25} evaluation

Samples of the equilibrium solution were taken out
and the readings on the refractometer were:

118.44, 118.50, 118.46, 118.47 : average 118.47

Therefore the refractive index was $n_D^{25} = 1.40416$

$x_1^l = 0.2704$ This was read on the calibration curve
corresponding to the value of $n_D^{25} = 1.40416$
The curve was plotted on a large chart
and was not shown in this thesis.

$$\begin{aligned}\Delta x_1^l &= x_1^o - x_1^l \\ &= 0.3097 - 0.2704 \\ &= 0.0393\end{aligned}$$

$$\frac{x_1^l x_2^l}{n^o \frac{\Delta x_1^l}{m}} = \frac{(0.3097)(0.6903)}{(0.08936)(0.0393)/2.1127} = 118.684$$

From the plot on Fig. 14 we obtained:

$$\frac{m}{n^o} \left(\frac{1}{K-1} \right) = \text{intercept} = 41.4$$

$$\frac{m}{n^o} = \text{slope} = 284.1$$

Solving the above simultaneous equations, we obtained:

$$K = 7.86$$

$$n^o = 0.007436$$

Hence x_1^{σ} could be calculated:

$$\begin{aligned}x_1^{\sigma} &= x_1^l + (x_1^o - x_1^l)(n^o/n^{\sigma}) \\ &= 0.2704 + (0.3097 - 0.2704)(0.08936/0.007436) \\ &= 0.7427\end{aligned}$$

$$x_2^{\sigma} = 1 - x_1^{\sigma} = 1 - 0.7427 = 0.2573$$

From Appendix I , we had $\gamma_1^l = 1.373$ $\gamma_2^l = 1.049$

Then the activity coefficients in the adsorbed phase could be calculated,

$$\begin{aligned} \ln \gamma_2^\sigma &= x_1^\sigma \ln \left(\frac{x_1^\sigma x_2^l \gamma_2^l}{x_2^\sigma x_1^l \gamma_1^l} \right) - \int_0^{x_1^\sigma} \ln \left(\frac{x_1^\sigma x_2^l \gamma_2^l}{x_2^\sigma x_1^l \gamma_1^l} \right) dx_1^\sigma \\ &= 0.0555 \end{aligned}$$

the detailed calculations was shown in Appendix II.

Using the same procedures , we had

$$\ln \gamma_1^\sigma = 0.0666$$

Finally, using graphical integration as shown in Appendix II ,

$$\begin{aligned} \ln K' &= \int_0^1 \ln \left(\frac{x_1^\sigma x_2^l \gamma_2^l}{x_2^\sigma x_1^l \gamma_1^l} \right) dx_1^\sigma \\ &= 1.7910 \\ K' &= 5.99 \end{aligned}$$

x_1	m	n°	n_D^{25}	$\frac{1}{x_1}$	$\frac{x_1^2 x_2^2}{(n^\circ \Delta x/m)}$	$\frac{\sigma}{x_1}$	$\ln \gamma_1^\sigma$	$\ln \gamma_2^\sigma$	K'
0.2005	2.4178	0.06579	1.38544	0.1562	109.34	0.6037	0.1321	0.1541	5.78
0.3008	2.7912	0.09447	1.39498	0.2612	143.98	0.7587	0.0799	0.2460	
0.3882	2.3223	0.09985	1.40482	0.3578	175.80	0.8430	0.0451	0.3875	
0.5098	2.7722	0.06666	1.41620	0.4596	205.76	0.9077	0.0114	0.6462	
0.5968	3.1276	0.10487	1.42901	0.5691	264.03	0.9139	0.0382	0.4299	
0.6958	3.5221	0.11781	1.44295	0.6735	294.81	0.9504	0.0087	0.6752	
0.8029	2.6253	0.12841	1.46101	0.7940	375.73	0.9693	0.0053	0.7365	
0.8944	2.7003	0.12089	1.47680	0.8850	241.84	1.0412	0.0034	0.7111	

Table 5

Liquid phase adsorption at 25°C for the system benzene-n-hexane-silica gel

x_1°	m	n°	n_D^{25}	x_1^l	$\frac{\rho_1 \rho_2}{x_1 x_2} \frac{1}{(n^\circ \Delta x_1^l / m)}$	x_1^σ	$\ln \gamma_1^\sigma$	$\ln \gamma_2^\sigma$	K'
0.1115	1.9429	0.05874	1.38964	0.0713	54.48	0.4166	0.0526	0.0257	5.99
0.2056	2.7489	0.08253	1.39551	0.1568	90.24	0.5730	0.1293	-0.0399	
0.3097	2.1127	0.08936	1.40416	0.2704	118.68	0.7427	0.0666	0.0555	
0.4289	1.7398	0.10362	1.41509	0.4010	144.55	0.8732	0.0074	0.3881	
0.6174	1.9536	0.10405	1.43504	0.5961	212.23	0.9184	0.0231	0.3384	
0.6883	3.1721	0.11249	1.44323	0.6612	233.10	0.9342	0.0139	0.3293	
0.8296	3.0756	0.10840	1.46452	0.8140	275.37	0.9702	0.0061	0.5932	
0.9014	2.1747	0.08550	1.47751	0.8930	289.33	0.9868	0.0002	0.9248	

Table 6

Liquid phase adsorption at 25°C for the system benzene-n-heptane-silica gel

x_1^0	m	n°	n_D^{25}	x_1^l	$\frac{x_1^l x_2^l}{(n^\circ \Delta x_1^l/m)}$	x_1^g	$\ln \gamma_1^g$	$\ln \gamma_1^l$	$\ln \gamma_2^g$	K'
0.0656	1.4880	0.05335	1.39704	0.0331	27.47	0.3512	-0.1469	0.1801	5.88	
0.0900	2.3231	0.07388	1.39798	0.0517	40.80	0.3797	0.0712	0.0720		
0.1836	2.1367	0.07585	1.40271	0.1411	80.33	0.5530	0.2007	-0.3082		
0.2958	1.9294	0.08952	1.40980	0.2568	95.84	0.7508	0.0832	0.1333		
0.4096	2.6827	0.09115	1.41635	0.3526	117.87	0.8813	0.0047	0.5881		
0.5924	3.4284	0.08810	1.43180	0.5397	183.25	0.9098	0.0345	0.3342		
0.6957	1.4977	0.07551	1.44553	0.6687	220.06	0.9436	0.0290	0.3654		
0.8007	1.7477	0.11332	1.46085	0.7800	228.19	0.9853	-0.0043	1.3366		

Table 7

Liquid phase adsorption at 25°C for the system benzene-n-octane-silica gel

x_1^0	m	n°	n_D^{25}	x_1^l	$\frac{x_1^l x_2^l}{(n^\circ \Delta x_1^l/m)}$	$\frac{\sigma}{x_1^l}$
0.1109	2.8030	0.05850	1.41152	0.0518	39.82	0.3577
0.2288	2.7559	0.06405	1.41574	0.1661	95.05	0.5275
0.2954	3.7025	0.06634	1.41777	0.2111	110.26	0.5357
0.4988	2.1860	0.08686	1.4311	0.4628	173.80	0.8175
0.5921	2.8259	0.08068	1.43753	0.5528	220.33	0.8311
0.6821	2.6399	0.09004	1.44616	0.6508	212.88	0.9156
0.7967	2.7779	0.10976	1.46019	0.7778	231.43	0.9630

Table 8

Liquid phase adsorption at 25°C for the system benzene-n-decane-silica gel

DISCUSSIONS

The values of the separation factor K' evaluated in this investigation are:

- 5.78 for the system benzene-n-hexane-silica gel
- 5.99 for the system benzene-n-heptane-silica gel
- 5.88 for the system benzene-n-octane-silica gel

This indicates that the difference of molecular size on these n-alkanes has little effect on the separation factor K' . Hence this leads to a suggestion that the adsorption of these n-alkanes on silica gel is independent of their chain lengths. Also this helps us to understand that the molecules of these n-alkanes are adsorbed onto the surface of the silica gel in such a manner that the point of contact is likely to be the two ends of the open chain. With a molecule of closed chain such as cyclohexane, the manner of being adsorbed is different and hence the reported K' was 10.47⁽³³⁾, which is very different from 5.78, 5.99 or 5.88.

If we compare the values of K , evaluated by assuming

perfect systems, with the values of K' which were evaluated with considerations of deviations,

<u>K</u>	<u>K'</u>	<u>system</u>
9.07	5.78	benzene-n-hexane-silica gel
7.86	5.99	benzene-n-heptane-silica gel
11.46	5.88	benzene-n-octane-silica gel
5.32	--	benzene-n-decane-silica gel

it is observed that the very different values of K are modified to values of K' which are close in magnitude. K' is not evaluated for the system benzene-n-decane-silica gel because the $\log \gamma^L$ values for this system are not available.

The evaluated $\log \gamma^{\sigma}$ values, as shown graphically in figures 21, 22 and 23, together with those for the system benzene-cyclohexane-silica gel reported by Lu and Lama⁽³³⁾, reveal a similar shape on plots of $\log \gamma^{\sigma}$ against x_1^{σ} . These curves are different from those for liquid phases, but they show that deviations from ideal do exist in the adsorbed phase. However, in the regions where x_1^{σ} is less than 0.4, extrapolation

methods ⁽⁴¹⁾ have to be used to obtain values for $\log \delta$.
Therefore an improved method to obtain experimental
data in these regions is desirable.

CONCLUSIONS

The binary liquid system carbontetrachloride-tetrachloroethylene is better realized as a system close to ideal when the heats of mixing data were evaluated at 25° C. It was found that the excess enthalpy of mixing is in the order of 15 cal./mole. This result, together with the excess free energy of mixing evaluated from vapor-liquid equilibrium data (in the order of 100 cal./mole), suggests that the imperfectness of this system is due to both the enthalpy of mixing and the entropy of mixing.

The principle of solubility parameter⁽¹⁶⁾ is tested with the help of the experimental $\Delta\tilde{H}^M$ data for the system carbontetrachloride-tetrachloroethylene at 25° C, such that the solubility parameter of carbontetrachloride is obtained in good agreement with the literature⁽³⁾.

For liquid phase adsorption, the activity coefficients in the adsorbed phase were evaluated for the 3 systems: benzene-n-hexane-silica gel, benzene-n-heptane-silica gel and benzene-n-octane-silica gel. The curves of $\log \gamma^{\sigma}$ for these systems are similar to that for the

system benzene-cyclohexane-silica gel, all at 25° C. (33)
The evaluated separation factors for these systems show
that the adsorption is independent of the chain lengths
of these n-alkanes.

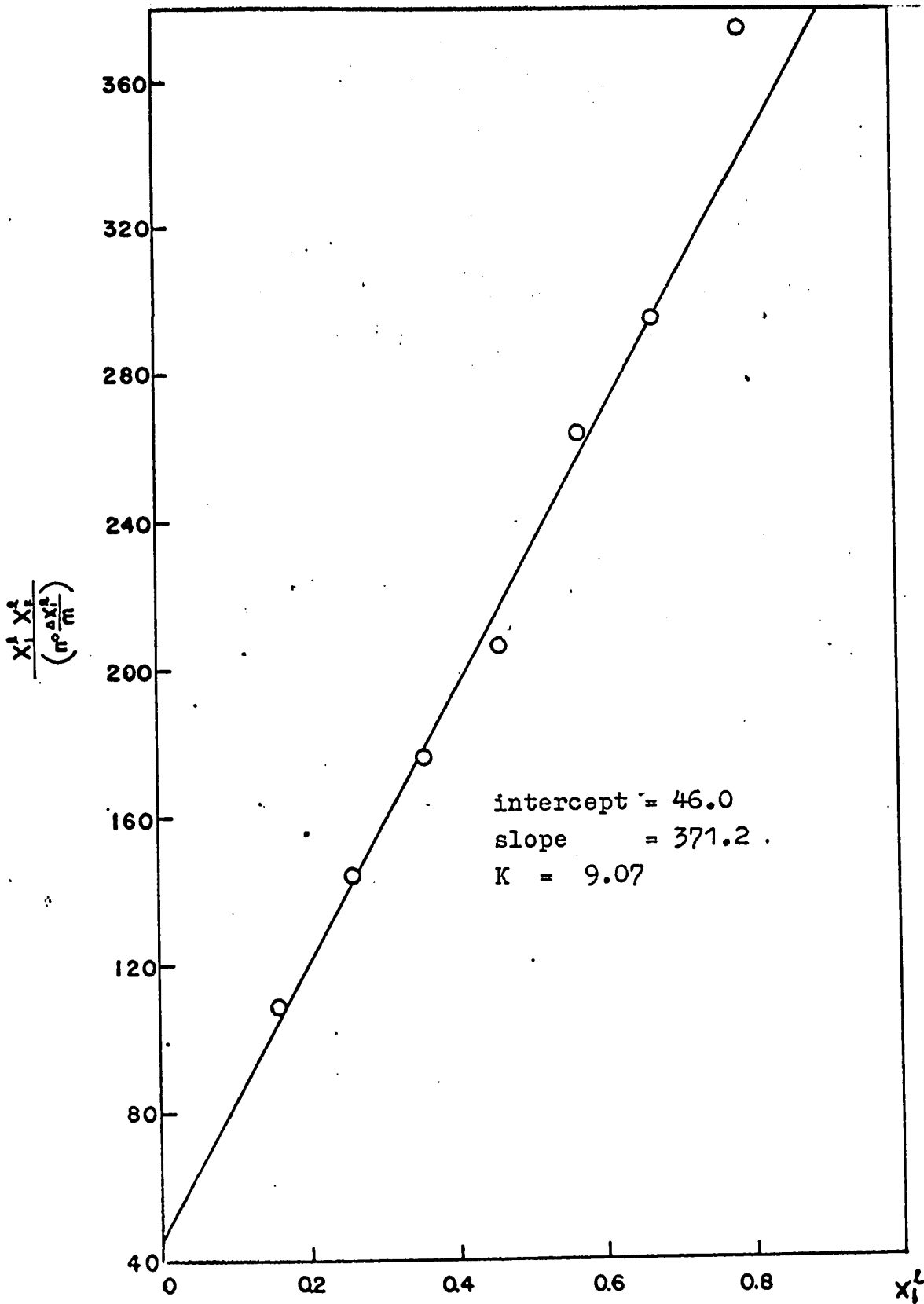


Fig.13 Equilibrium adsorption at 25°C
System Benzene-n-hexane-silica gel

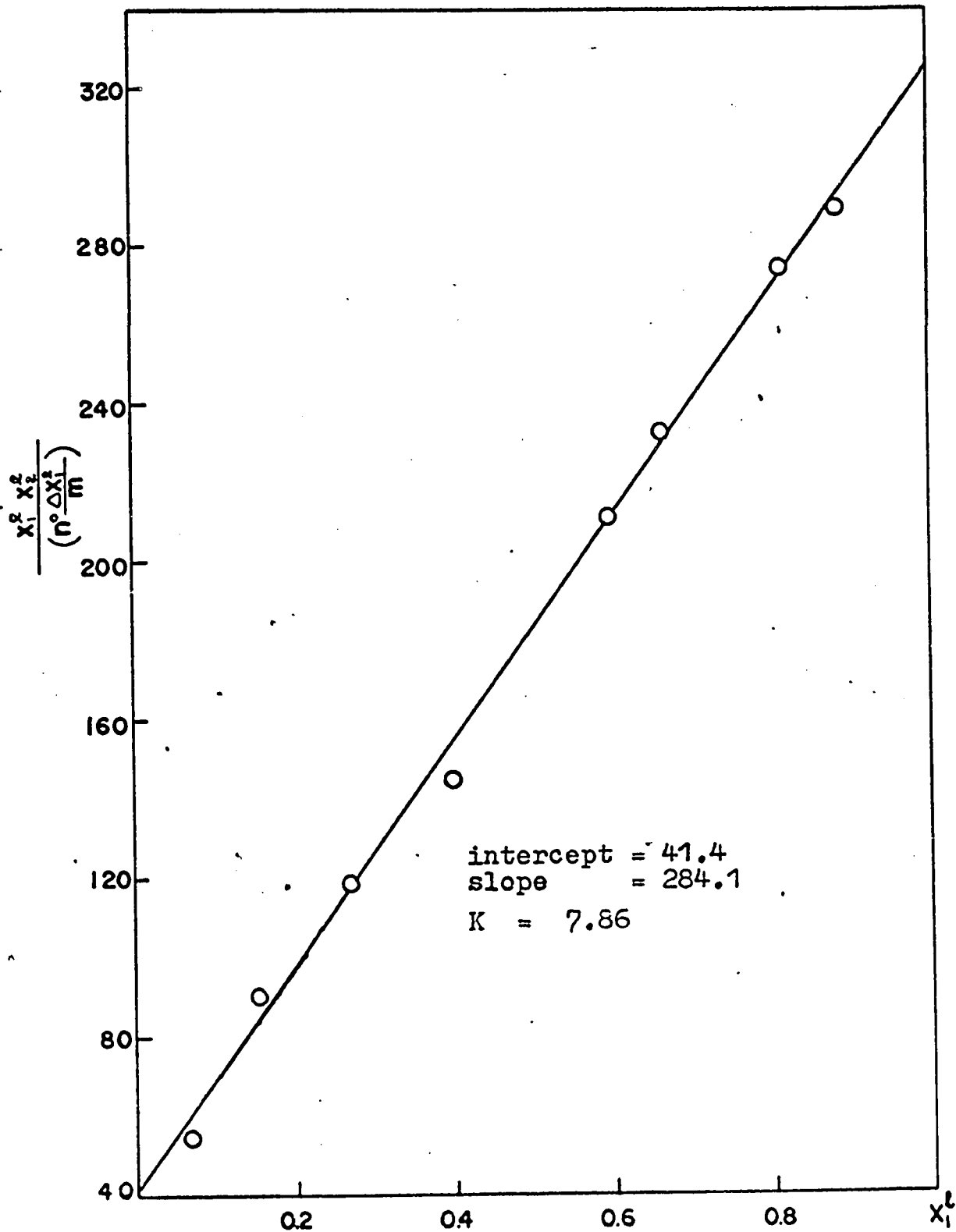


Fig.14 Equilibrium adsorption at 25°C
System benzene-n-heptane-silica gel

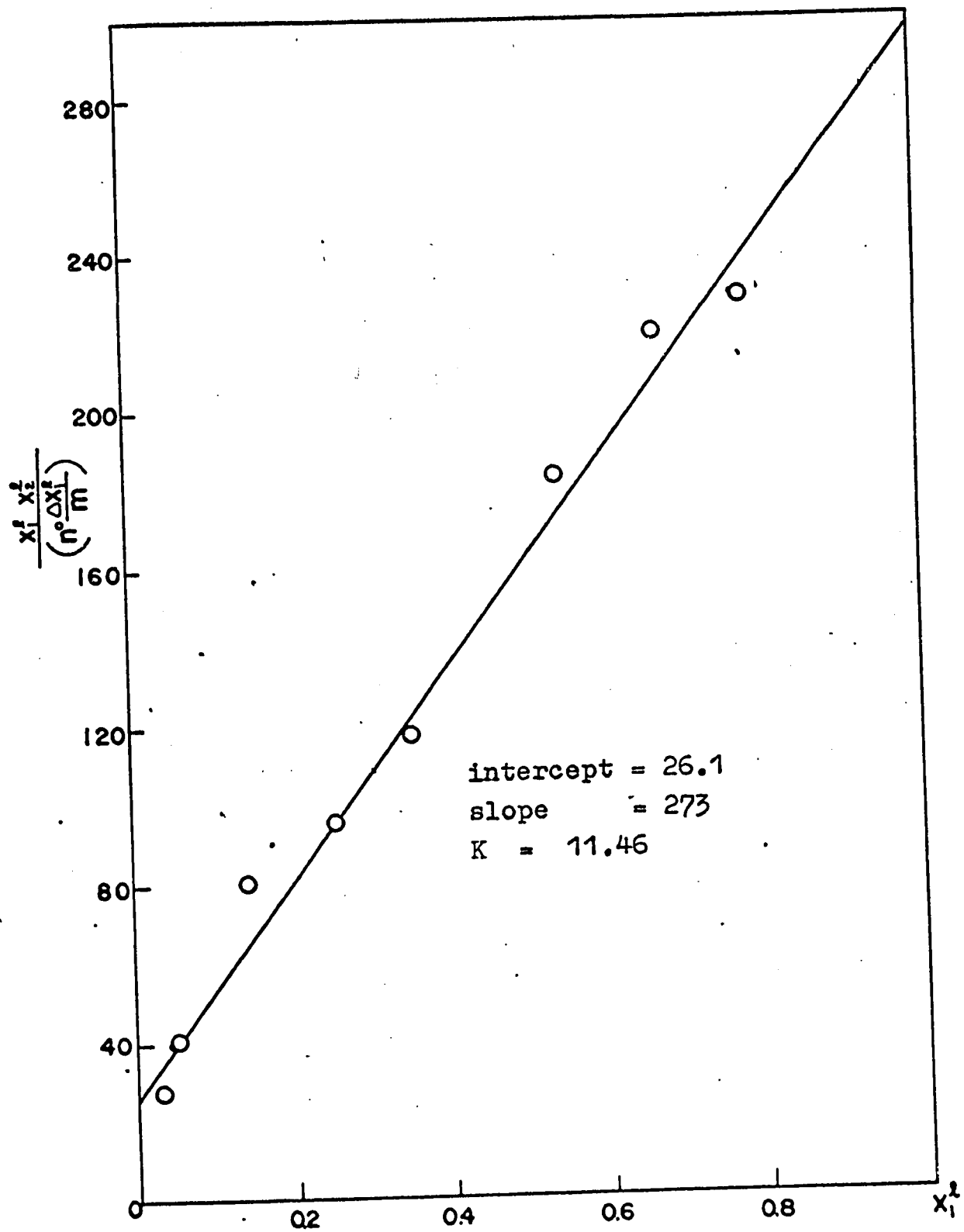


Fig.15 Equilibrium adsorption at 25° C
System : benzene-n-octane-silica gel

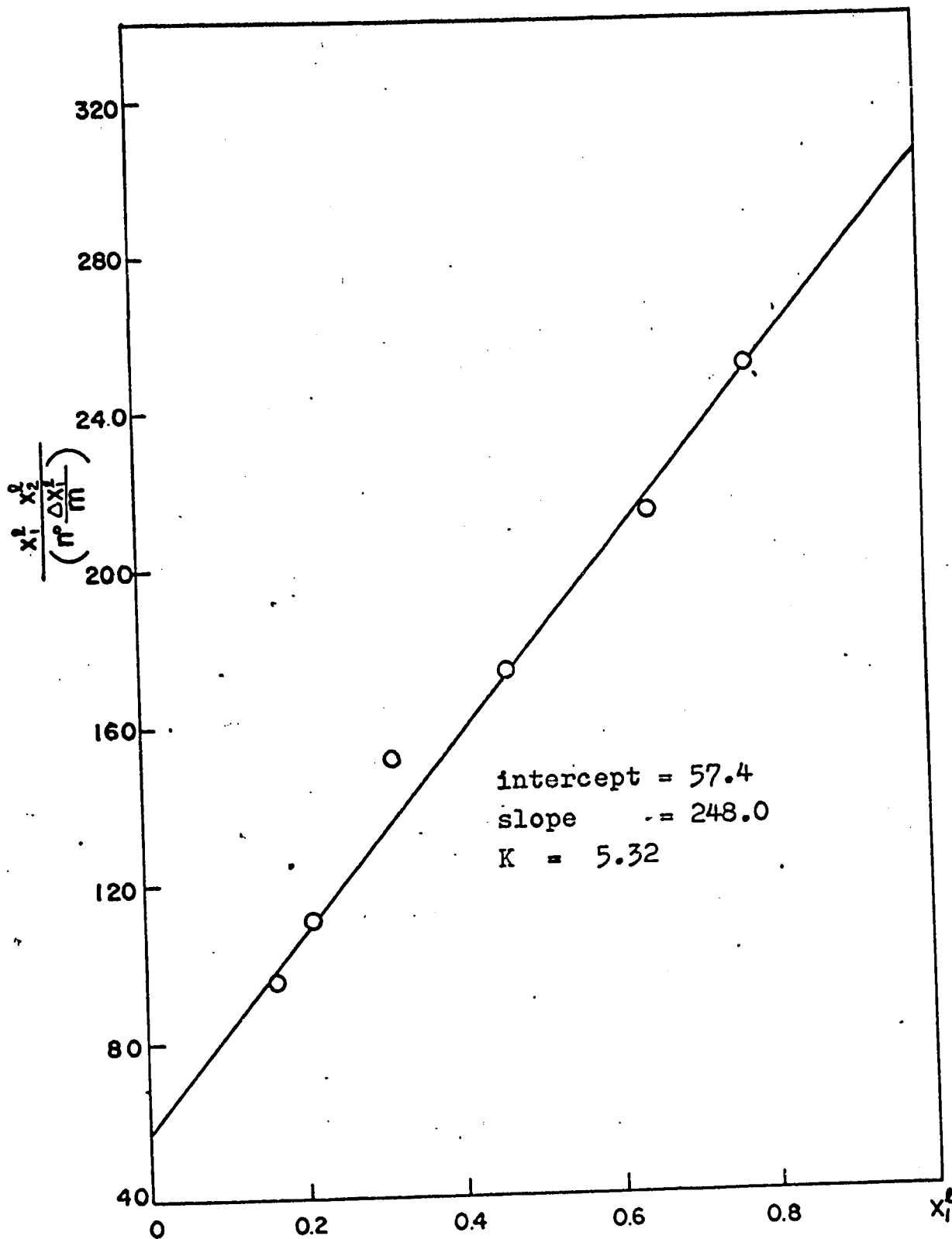


Fig.16 Equilibrium adsorption at 25°C
System: benzene-n-decane-silica gel

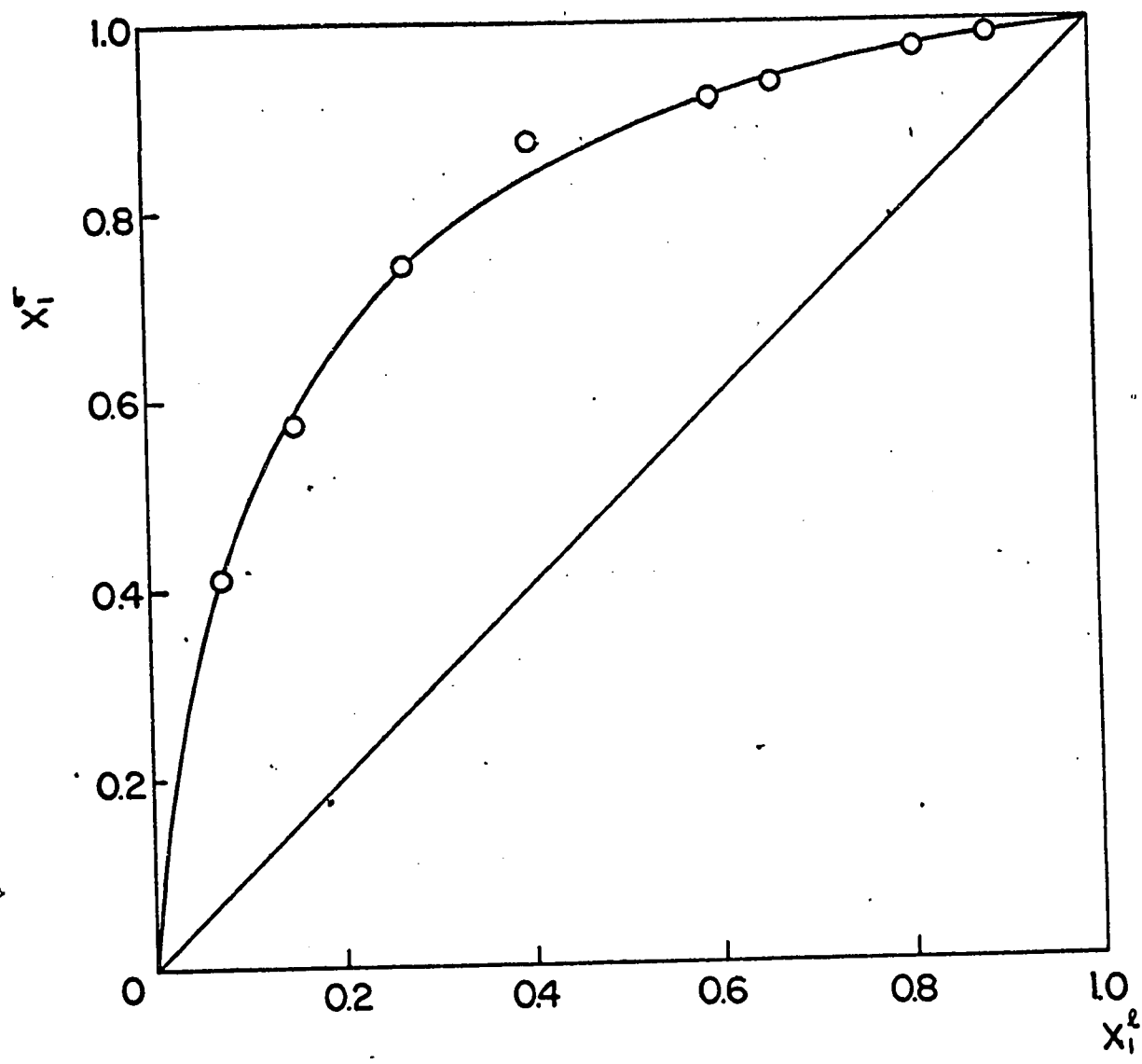


Fig.17 Equilibrium $x_1^\sigma - x_1^l$ diagram (25°C)

System: benzene-n-hexane-silica gel

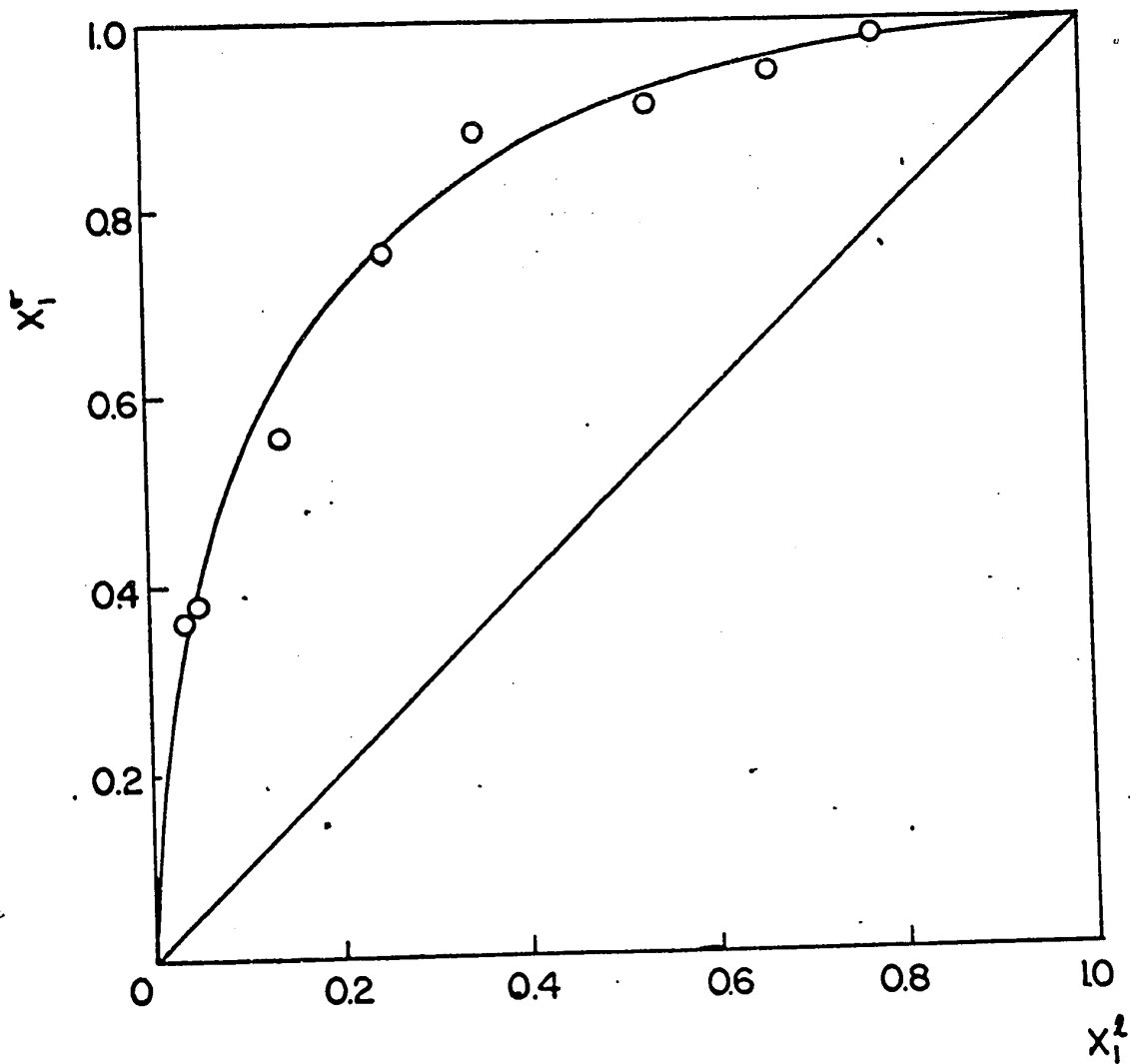


Fig.18: Equilibrium $x_1^\sigma - x_1^l$ diagram (25°C)
System: benzene-n-heptane-silica gel

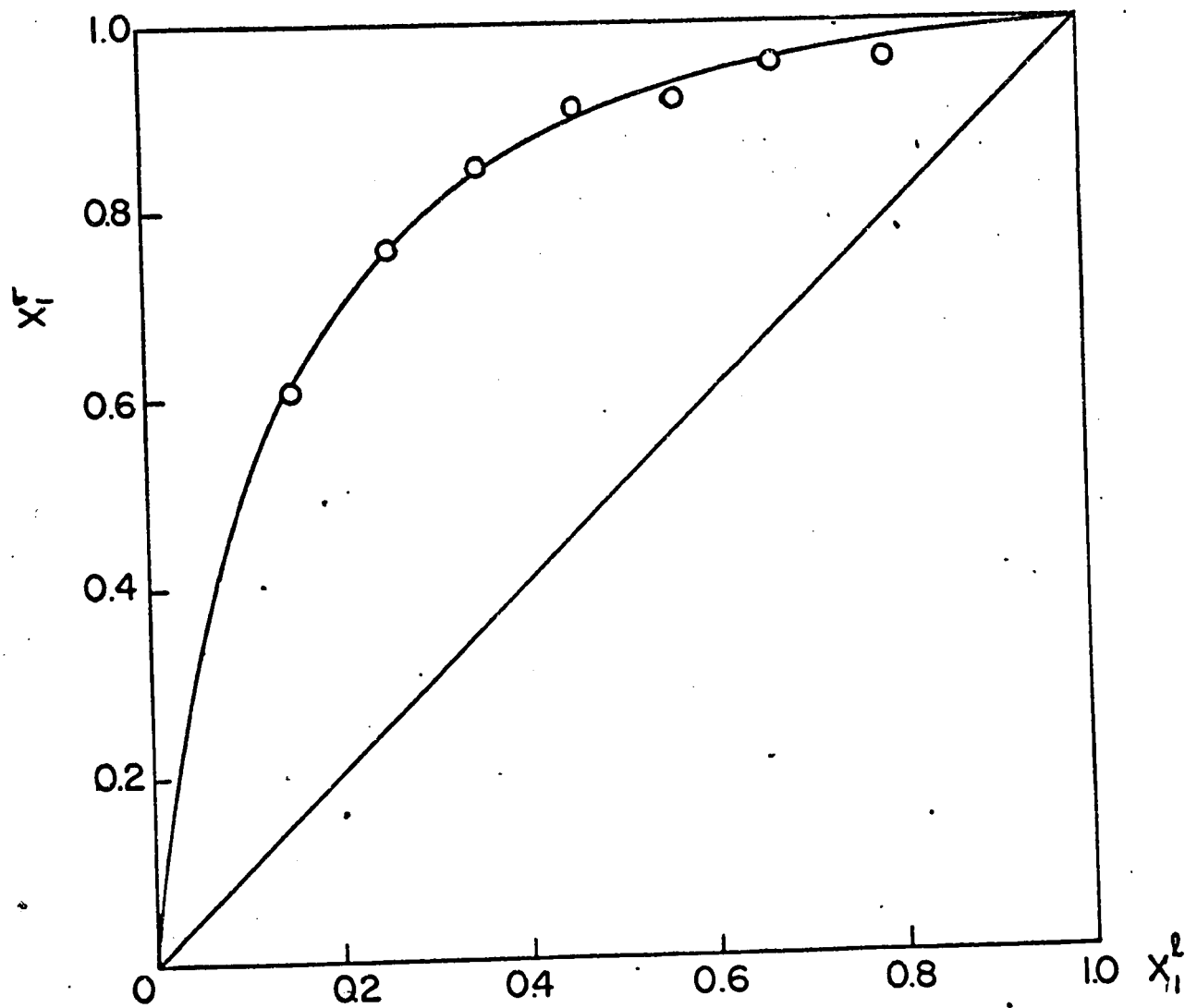


Fig.19 Equilibrium $x_1^\sigma - x_1^l$ diagram (25°C)
System: benzene-n-octane-silica gel

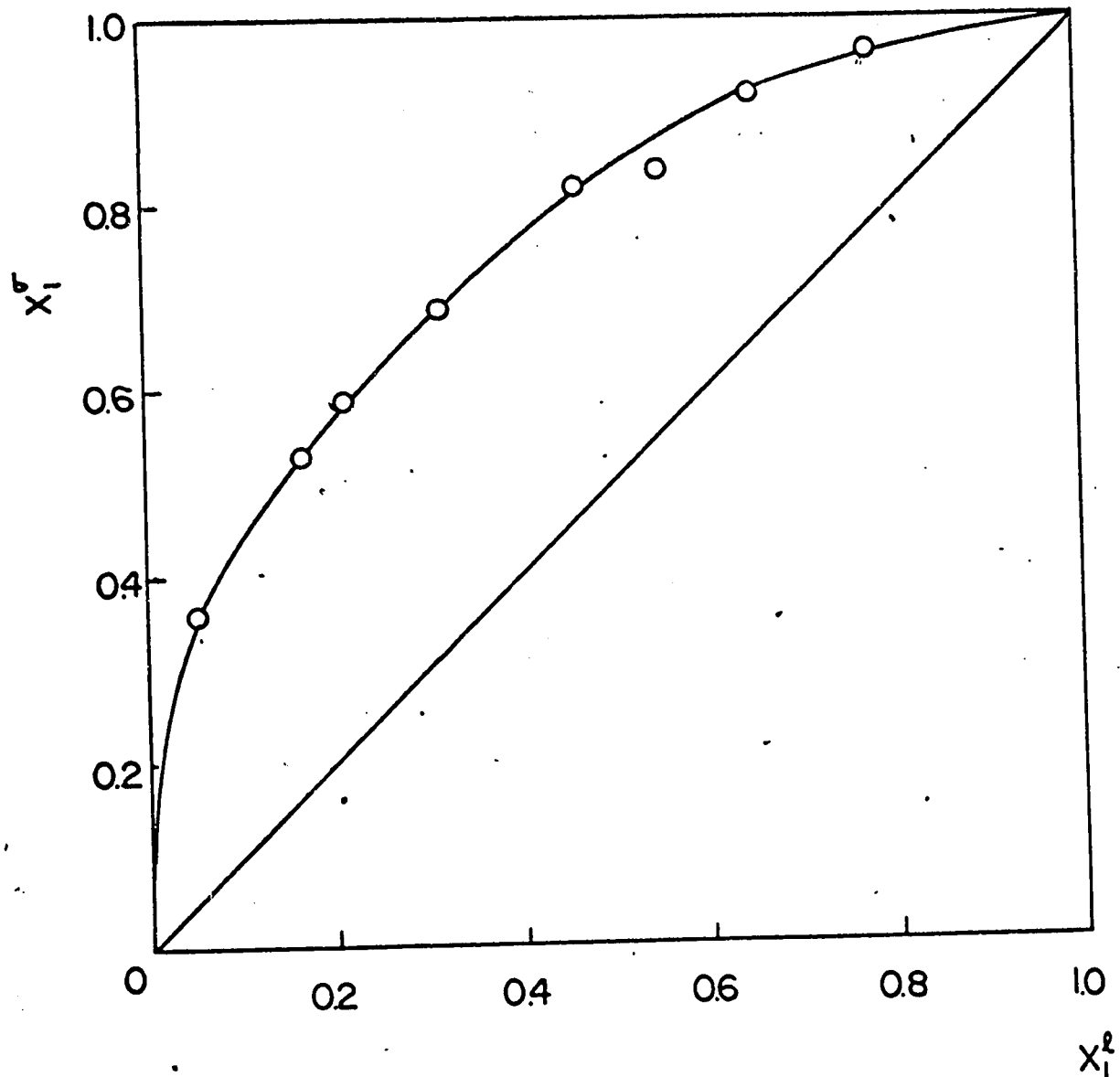


Fig.20 Equilibrium $x_1^\sigma-x_1^l$ diagram (25°C)
System: benzene-n-decane-silica gel

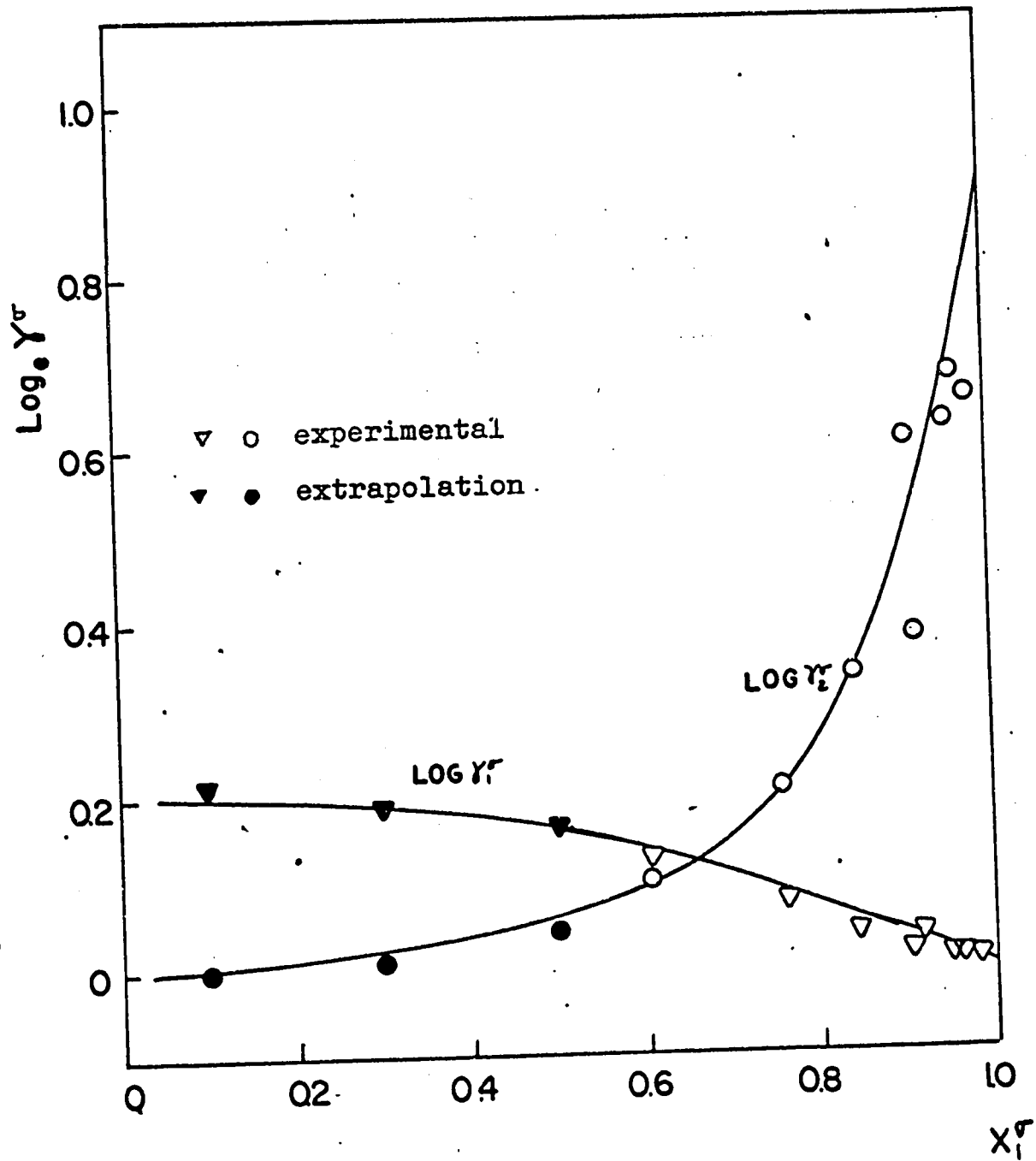


Fig.21 Calculated $\text{log}_e Y_i^\sigma$ values as a function of x_1^σ
System: benzene-n-hexane-silica gel (25° C)

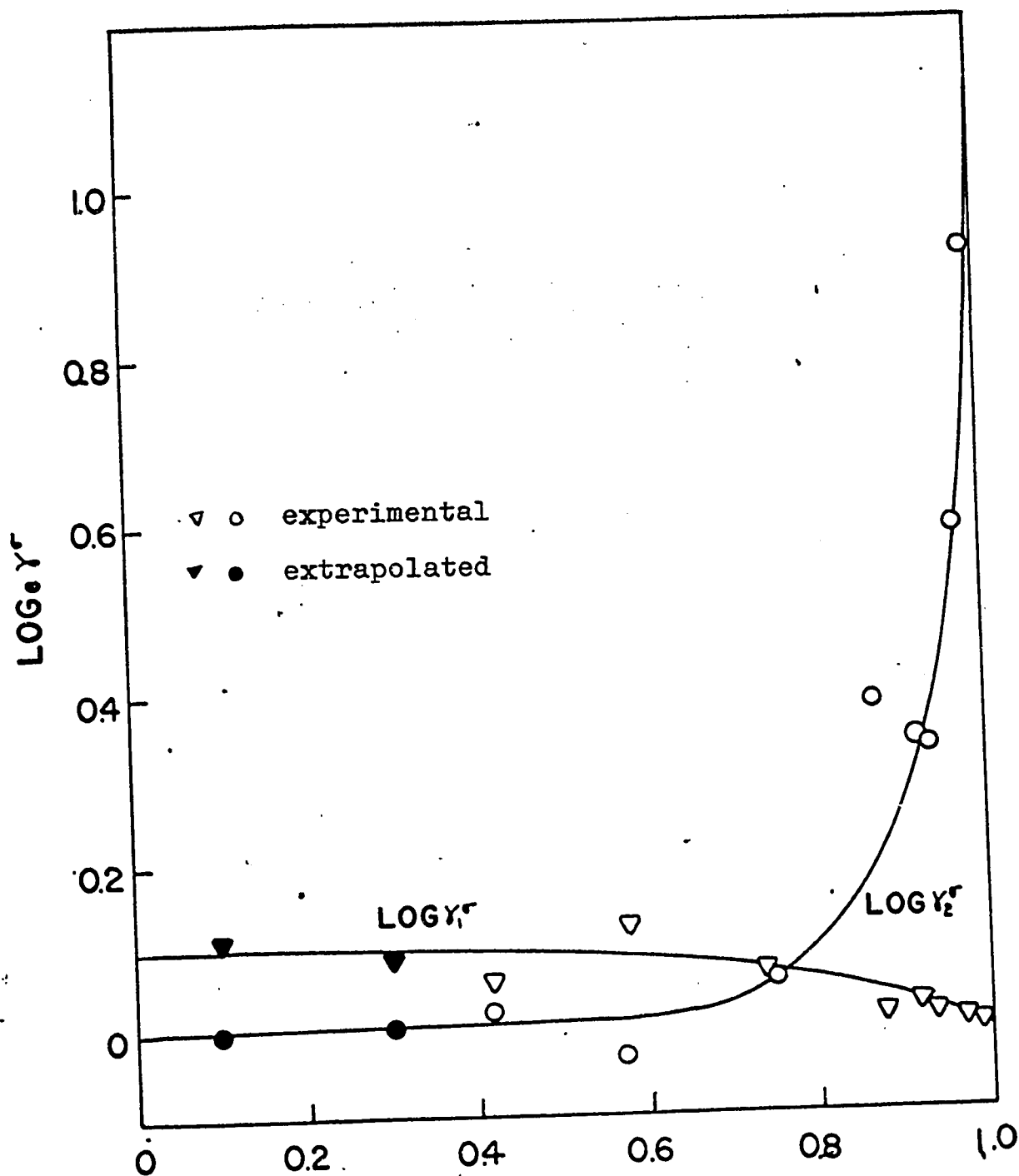


Fig.22 Calculated $\text{log}_e Y^{\sigma}$ values as a function of X_1^{σ}
System: benzene-n-heptane-silica gel (25°C)

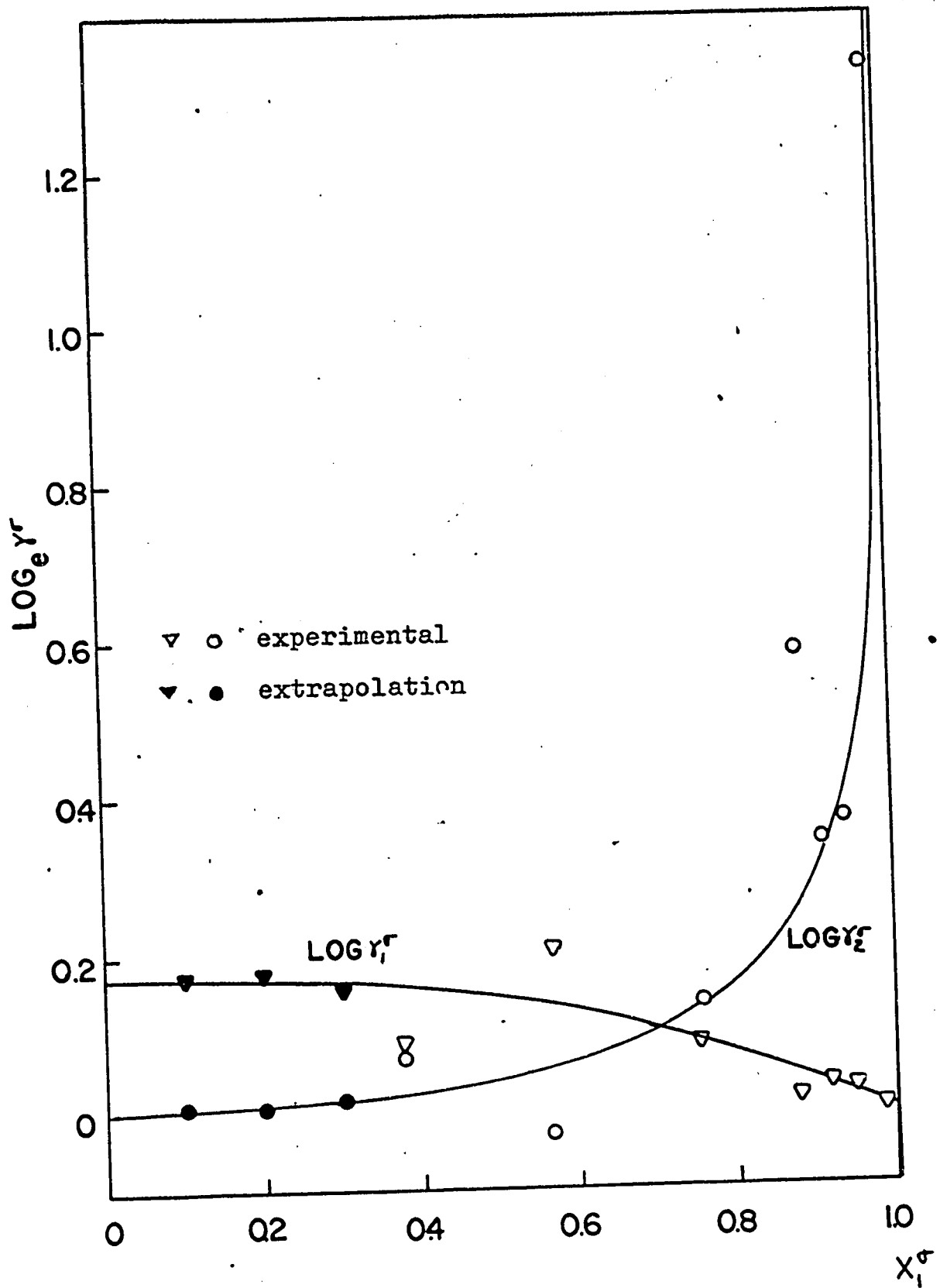


Fig.23 Calculated $\log_e \gamma^{\sigma}$ values as a function of x_1^{σ}
System: benzene-n-octane-silica gel (25°C)

LITERATURE SITED

- (1) Subbarao, B.V. and Venkatarao, C., Canadian J. of Chem. Eng. Vol.43, No.6, 289 (1965).
- (2) Jones, H.K.D., Poon, D., Lama, R.F. and Lu, B.C.Y., Canadian J. of Chem. Eng., Vol.45, No. ,22,(1967).
- (3) Hildebrand, J.H. and Scott, R.C., "The solubility of nonelectrolytes" Dover Publications, New York, page 436, (1964).
- (4) Everett, D.H., Trans. Far. Soc., 60, 1803, (1964).
- (5) Lu, B.C.Y., Canadian J. of Chem. Eng., October, 193, (1959).
- (6) Richards, T.W., Proc. Am. Acad., 41, 11, (1905).
- (7) Carroll, B.H. and Mathews, J.H., J. Amer. Chem. Soc., 46, 30, (1934).
- (8) Macleod, D.B. and Wilson, F.J., Tran. Far. Soc., 31, 569, (1935).
- (9) Vold, R.D., J. Amer. Chem. Soc., 59, 1515 (1937).
- (10) Scatchard, G., Ticknor, L.B., Goates, J.R. and McCartney, E.R., J. Amer. Chem. Soc., 74, 3221 (1952).
- (11) Tsao, C.C. and Smith, J.M., Chem. Eng. Prog. Symp. Series No.7, 49, 107 (1953).
- (12) Hanson, D.O. and Van Winkle, M., J. Chem. and Eng. Data, Vol.5, No.1, 30 (1960).
- (13) Lama, R.F. and Lu, B.C.Y., J. of Chem. and Eng. Data, Vol.10, No.3, 216 (1965).

- (14) Brunauer, S., Emmett, P.H. and Teller, E., J. Am. Chem. Soc., 60, 309(1938).
- (15) Brown, I., Australian J. Sc. Research, 5A, 536(1952).
- (16) Hildebrand, J.H. and Scott, R.C., "The solubility of nonelectrolytes" Dover Publications, New York, page 129 (1964).
- (17) Hildebrand, J.H. and Scott, R.C., "The solubility of nonelectrolytes", Dover Publications, New York, page 424 (1964).
- (18) Dreisbach, R.R., "Physical properties of chemical substances" , The Dow Chemical Company, Handbook Publishers Inc., (1953).
- (19) Kipling, J.J., Proc. Int. Cong. Surface Activity, 3rd, Cologne, 2, 77, (1961).
- (20) Nagy, L.G. and Schay, G., Acta Chim. Hung., 39, 365(1963)
- (21) Kiselev, A.V. and El tekov, Y.A., Dokl. Akad. Nauk SSSR, 100, 107(1955).
- (22) Kiselev, A.V., Proc. Int. Cong. Surface Activity, 2nd, London, 2, 179(1957).
- (23) Jones, H.L. and Stuart, E.B., A.I.Ch.E. Journal, 6, 332(1960).
- (24) Kiselev, A.V. and Pavlova, L.F., Neftekhimiya, 2, 861(1962).
- (25) Bartell, F.E. and Sloan, C.K., J. Am. Chem. Soc., 51, 1637 and 1643 (1929).
- (26) Kipling, J.J. and Tester, D.A., J. Chem. Soc., 4123(1952).

- (27) Elton, J., J.Chem.Soc., 2958 (1951).
- (28) Schiessler, R.W. and Rowe, C.N., J.Am.Chem.Soc., 76, 1202, (1954).
- (29) Siskova, M. and Erdos, E., Collection Czech. Chem. Commun, 25, 1729 (1960) and 26, 3086 (1961).
- (30) Cleland, R.I., J.Phy.Chem., 68, 1432 (1964).
- (31) Lu, B.C.Y. and Lama, R.F., Trans.Far.Soc., 2478 (1965).
- (32) Brown, I. and Ewald, A.H., Australian J.Sc. Research, 4A, 198 (1951).
- (33) Lu, B.C.Y. and Lama, R.F., Tran.Far.Soc., Vol.63, 727 (1967).
- (34) Bartell, F.E. and Suggitt, R.M., J.Phy.Chem., 58, 36 (1954).
- (35) Lama, R.F. and Lu, B.C.Y., J.of Chem. and Eng.Data, Vol.11, No.1, 47 (1966).
- (36) Savini, C.G., Winterhalter, D.R., Kovach, L.H. and Van Ness H.C., J.of Chem. and Data, Vol.11, No.1, 40 (1966).
- (37) Lama, R.F., Ph.D. Thesis, Chem. Eng., U. of Ottawa, Canada (1965).
- (38) Harkins, W.D. and Boyd, G.E., J.Am.Chem.Soc., 64, 1195 (1942).
- (39) Weissberger, A., "Technique of organic chemistry" Vol.I, Physical Methods, part I, 2nd edition, Interscience Publishers Inc., N.Y., 743 (1949).
- (40) Lu, B.C.Y. and Jones, H.K.D., Canadian J. of Chem. Eng., october, 251 (1966).
- (41) Lu, B.C.Y., The Canadian J. of Chem.Eng., Oct.193 (1959).

APPENDIX I

Method of extrapolation for
activity coefficients in the liquid phase

Purpose: For the system benzene-n-heptane, vapor-liquid equilibrium data were available at 60° and 80° C. It was required that these data be extrapolated to 25° C.

Data: Heats of mixing data at 25° C by Jones, H.K.D. (40)
Vapor-liquid equilibrium data at 60° C by Brown (32)
Vapor-liquid equilibrium data at 80° C by Brown (15)

Method (5): Solving simultaneous equations:

$$L_1 = a + b T$$

$$\ln \gamma_1^{60} = c + a/RT - (b/R) \ln T$$

$$\ln \gamma_1^{80} = c + a/RT - (b/R) \ln T$$

the constants a, b and c could be evaluated.

With the evaluated a, b and c, activity coefficients at 25° C could be extrapolated by

using

$$\ln \gamma_1^{25} = c + a/RT - (b/R) \ln T$$

L_2 L_1
 I_1 I_2

Procedures:

$\Delta \hat{H}^M / x_1 x_2$ was plotted against x_1 , as shown in fig. 24, so that I_1 and I_2 were obtained.

By using $L_2 = \bar{H}_1 - \tilde{H}_1 = x_2^2 (2 \Delta \hat{H}^M / x_1 x_2 - I_1)$, L_2 was evaluated, eg. at $x_1 = 0.4$, $L_2 = 122.4$.

Similarly we had $L_1 = 334.0$.

$\ln Y$ was plotted against x_1 , as shown in fig.25,26. Values of $\ln Y$ were read at 0.1 intervals, eg. at $x_1=0.4$, $\ln Y_1^{60} = 0.1588$; $\ln Y_1^{80} = 0.1300$. This was done in a large graph and fig.25 was used to illustrate the procedure.

The values of the L_1 , L_2 , $\ln Y_1^{60}$, $\ln Y_2^{60}$, $\ln Y_1^{80}$ and $\ln Y_2^{80}$ are listed in Table (9). Using these values, 3 simultaneous equations were set up, and the constants a, b and c were evaluated; for example, at $x_1 = 0.4$,

$$334.0 = a + b(298)$$

$$0.1588 = c + a/(1.987)(333) - (b/1.987) \ln(333)$$

$$0.1300 = c + a/(1.987)(353) - (b/1.987) \ln(353)$$

solving these simultaneous equations, we obtained:

$$a = 111.59$$

$$b = 0.7696$$

$$c = 2.2401$$

The calculated values of a, b and c were substituted into

$$\begin{aligned} \ln Y_1^{25} &= c + a/(1.987)(298) - (b/1.987) \ln(298) \\ &= 0.2393 \end{aligned}$$

The calculated values of $\ln Y$ are listed in Table (9),

Table 9

Extrapolation of activity coefficients for the system
benzene-n-heptane, at 25°C.

<u>x₁</u>	<u>L₁²⁵</u>	<u>L₂²⁵</u>	<u>lnγ₁⁶⁰</u>	<u>lnγ₂⁶⁰</u>	<u>lnγ₁⁸⁰</u>	<u>lnγ₂⁸⁰</u>	<u>lnγ₁²⁵</u>	<u>lnγ₂²⁵</u>
0.1	745	-3	0.2500	0.0111	0.2410	0.0096	0.4339	0.0121
0.2	570	26.5	0.2223	0.0251	0.2040	0.0196	0.3633	0.0328
0.3	423	74.2	0.1913	0.0414	0.1680	0.0372	0.2959	0.0563
0.4	334	122.4	0.1588	0.0606	0.1300	0.0550	0.2393	0.0790
0.5	262	181.9	0.1235	0.0903	0.0968	0.0800	0.1881	0.1139
0.6	190	270.0	0.0869	0.1362	0.0617	0.0980	0.1396	0.1736
0.7	126	390.2	0.0547	0.2020	0.0397	0.1680	0.0897	0.2655
0.8	708	55.4	0.0283	0.2914	0.0200	0.2400	0.0493	0.3996
0.9	290	8.6	0.0082	0.3920	0.0061	0.3200	0.0152	0.5520

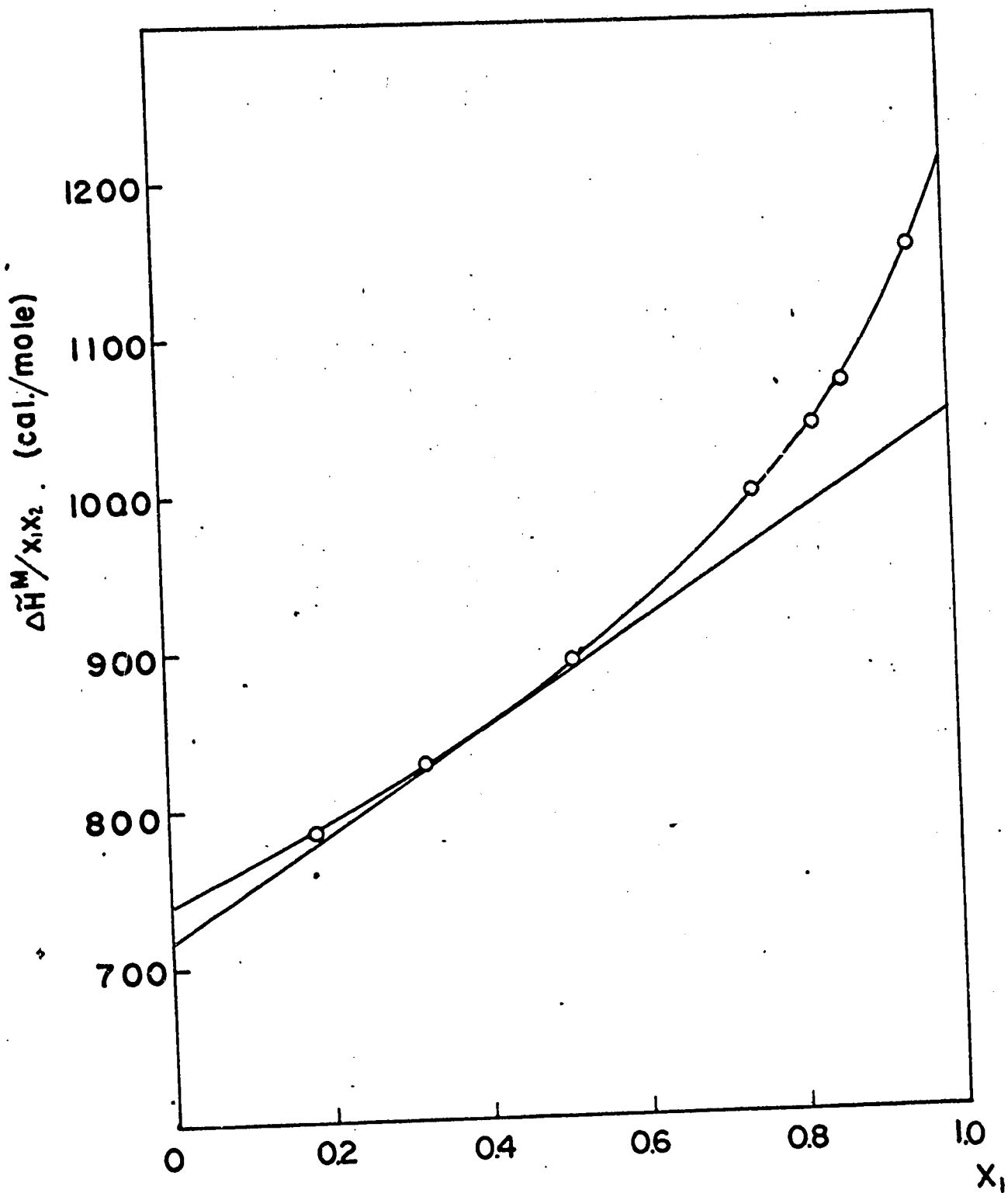


Fig.24 Heats of mixing data for the system benzene(1)-n-heptane(2), at 25°C. A plot of $\Delta \bar{H}^M / x_1 x_2$ against x_1 .

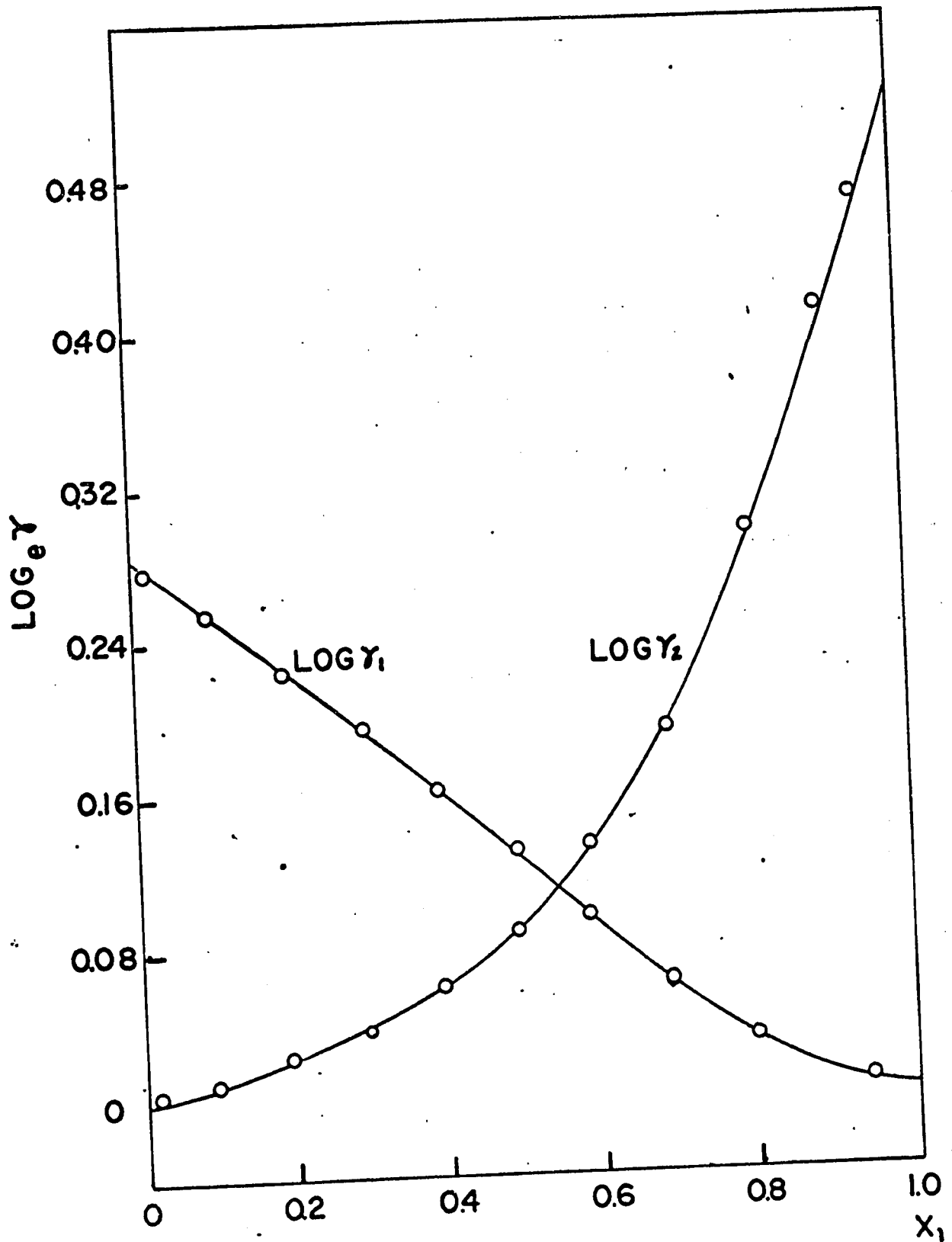


Fig.25 A plot of $\log_e \gamma$ against x_1 , for the system benzene(1)-n-heptane(2), at 60°C

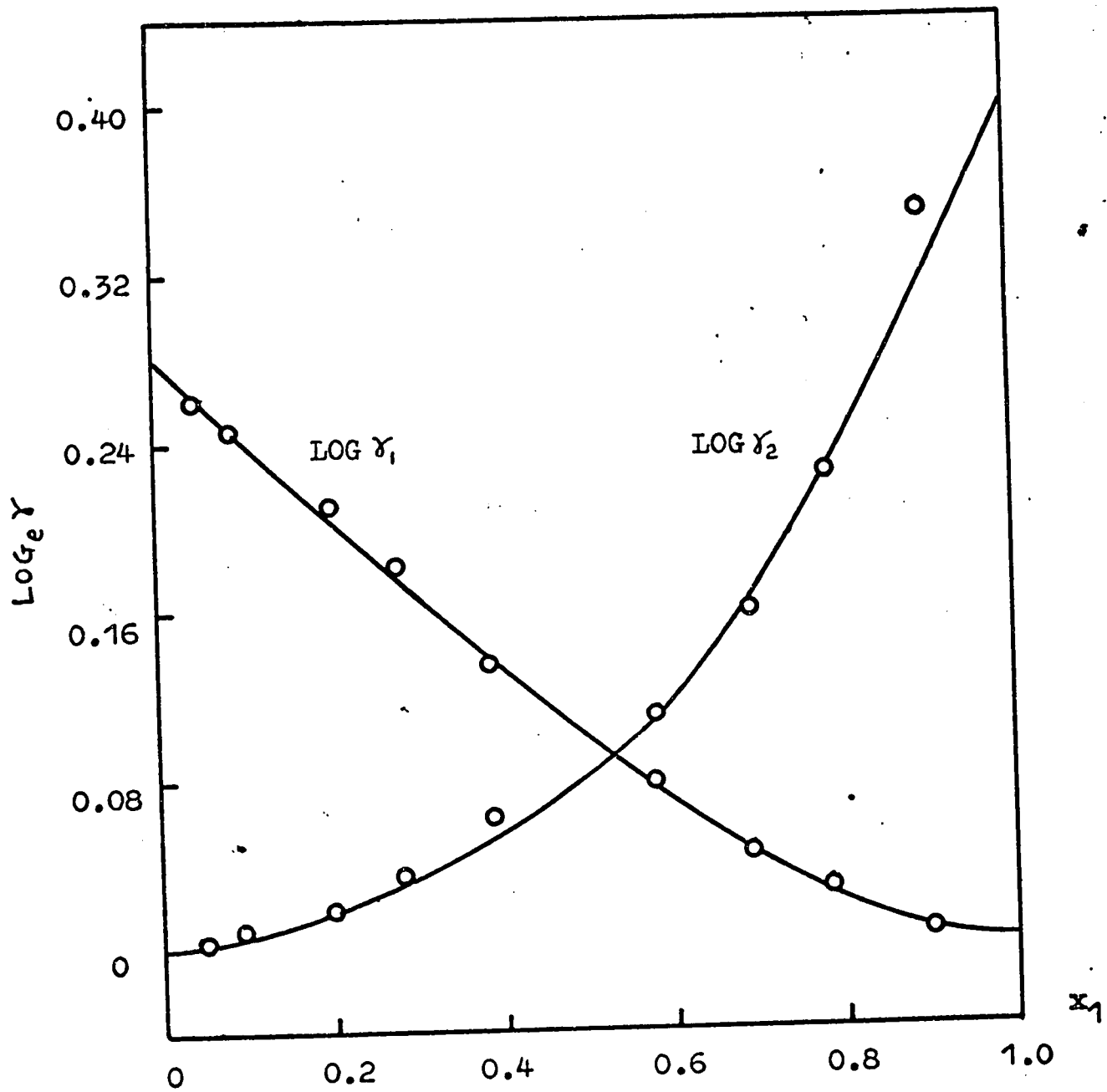


Fig.26 A plot of $\log_e \gamma$ against x_1 , for the system benzene(1)-n-heptane(2), at 80°C.

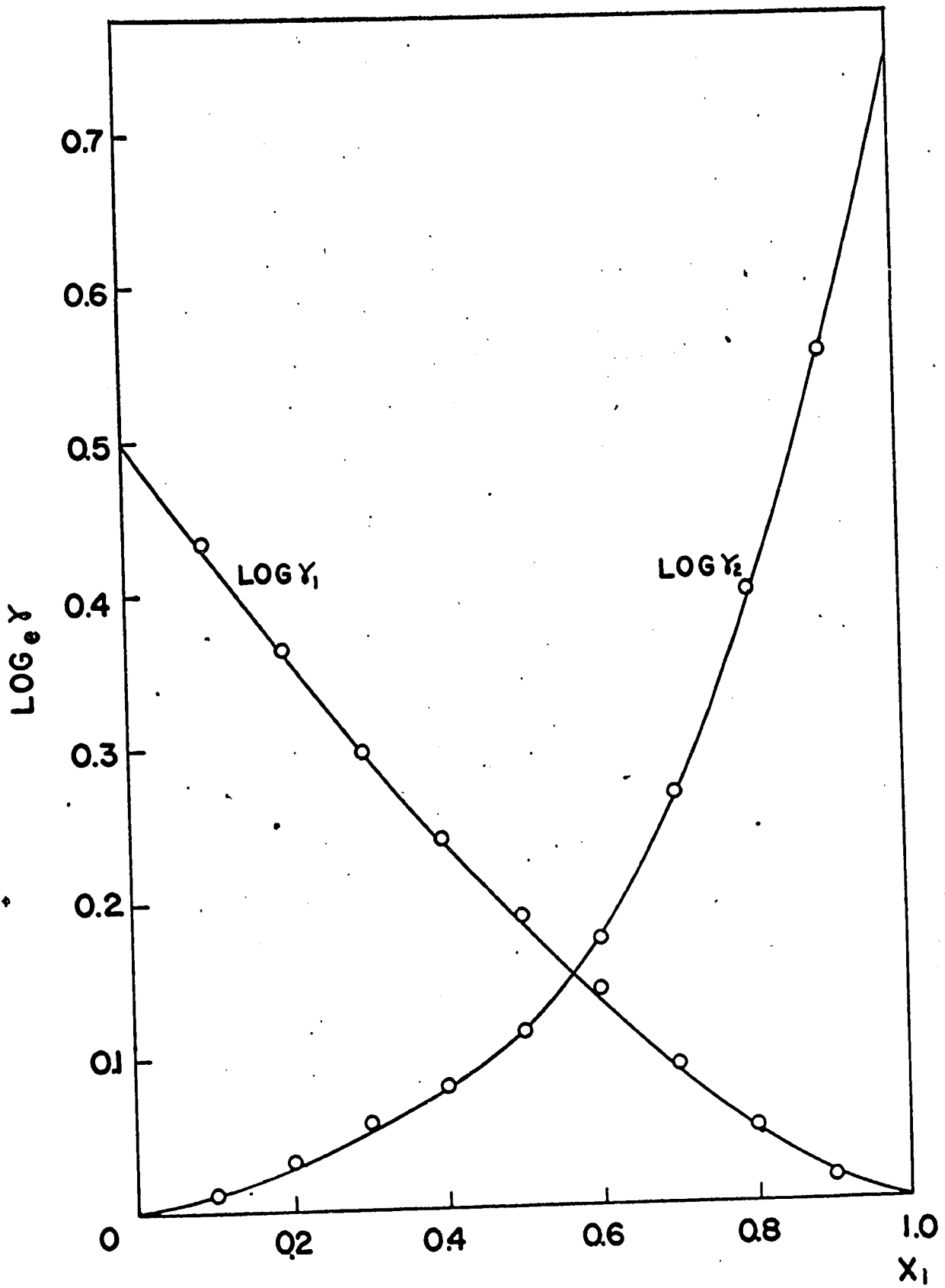


Fig.27 A plot of calculated $\log_e \gamma$ vs x_1 for the system benzene(1)-n-heptane(2), at 25°C

APPENDIX II

The method of evaluation
of activity coefficients in the adsorbed phase

The equations used were:

$$\ln Y_1^\sigma = x_2^\sigma \ln\left(\frac{x_2^\sigma x_1^\ell \gamma_1^\ell}{x_1^\sigma x_2^\ell \gamma_2^\ell}\right) - \int_0^{x_2^\sigma} \ln\left(\frac{x_2^\sigma x_1^\ell \gamma_1^\ell}{x_1^\sigma x_2^\ell \gamma_2^\ell}\right) dx_2^\sigma$$

$$\ln Y_2^\sigma = x_1^\sigma \ln\left(\frac{x_1^\sigma x_2^\ell \gamma_2^\ell}{x_2^\sigma x_1^\ell \gamma_1^\ell}\right) - \int_0^{x_1^\sigma} \ln\left(\frac{x_1^\sigma x_2^\ell \gamma_2^\ell}{x_2^\sigma x_1^\ell \gamma_1^\ell}\right) dx_1^\sigma$$

The integrals were evaluated by graphical method.

Plots of

$$\ln\left(\frac{x_2^\sigma x_1^\ell \gamma_1^\ell}{x_1^\sigma x_2^\ell \gamma_2^\ell}\right) \quad \text{against } x_2^\sigma$$

$$\ln\left(\frac{x_1^\sigma x_2^\ell \gamma_2^\ell}{x_2^\sigma x_1^\ell \gamma_1^\ell}\right) \quad \text{against } x_1^\sigma$$

were constructed, and values of

$$\int_0^{x_2^\sigma} \ln\left(\frac{x_2^\sigma x_1^\ell \gamma_1^\ell}{x_1^\sigma x_2^\ell \gamma_2^\ell}\right) dx_2^\sigma \quad \text{and} \quad \int_0^{x_1^\sigma} \ln\left(\frac{x_1^\sigma x_2^\ell \gamma_2^\ell}{x_2^\sigma x_1^\ell \gamma_1^\ell}\right) dx_1^\sigma$$

were listed in Table 10

The values of $\ln Y_1^\sigma$ and $\ln Y_2^\sigma$ evaluated were listed in Table 10

x_2^σ	x_1^σ	x_1^l	x_2^l	γ_1^l	γ_2^l
0.5884	0.4116	0.0713	0.9287	1.575	1.007
0.4270	0.5730	0.1568	0.8432	1.479	1.021
0.2573	0.7427	0.2704	0.7296	1.373	1.049
0.1268	0.8732	0.4010	0.5990	1.270	1.081
0.0816	0.9184	0.5961	0.4039	1.145	1.181
0.0658	0.9342	0.6612	0.3388	1.110	1.260
0.0298	0.9702	0.8140	0.1860	1.047	1.520
0.0132	0.9868	0.8930	0.1070	1.017	1.716

x_1^σ	$\frac{x_2^\sigma x_1^l \gamma_1^l}{x_1^\sigma x_2^l \gamma_2^l}$	$\ln\left(\frac{x_2^\sigma x_1^l \gamma_1^l}{x_1^\sigma x_2^l \gamma_2^l}\right)$	$\int_0^{x_2^\sigma} \ln\left(\frac{x_2^\sigma x_1^l \gamma_1^l}{x_1^\sigma x_2^l \gamma_2^l}\right) dx_2^\sigma$	$\ln \gamma_1^\sigma$	$\ln \gamma_2^\sigma$
0.4116	0.1717	-1.7623	-1.0895	0.0526	0.0257
0.5730	0.2007	-1.6061	-0.8151	0.1293	-0.0399
0.7427	0.2126	-1.7700	-0.5220	0.0666	0.0555
0.8732	0.1142	-2.1701	-0.2826	0.0074	0.3881
0.9184	0.1271	-2.0630	-0.1914	0.0231	0.3384
0.9342	0.1211	-2.1116	-0.1582	0.0139	0.3293
0.9702	0.0926	-2.3799	-0.0770	0.0061	0.5932
0.9868	0.0662	-2.7155	-0.0360	0.0002	0.9248

Table 10 Values for evaluating the activity coefficients in the adsorbed phase.
System: benzene-n-heptane-silica gel